WILEY | Hindawi

Review Article

Powder Bed Fusion via Machine Learning-Enabled Approaches

Utkarsh Chadha [ID],[1,2] Senthil Kumaran Selvaraj [ID],[2] Abel Saji Abraham [ID],[2]
Mayank Khanna [ID],[2] Anirudh Mishra [ID],[3] Isha Sachdeva [ID],[4] Swati Kashyap [ID],[5]
S. Jithin Dev [ID],[2] R. Srii Swatish [ID],[2] Ayushma Joshi,[3] Simar Kaur Anand [ID],[3]
Addisalem Adefris [ID],[6] R. Lokesh Kumar,[3] Jayakumar Kaliappan [ID],[3] and S. Dhanalakshmi[7]

[1]*Department of Materials Science and Engineering, aculty of Applied Sciences and Engineering, University of Toronto, St. George Campus, Toronto, Ontario M5S 1A1, Canada*
[2]*Department of Manufacturing Engineering, School of Mechanical Engineering (SMEC), Vellore Institute of Technology, Vellore, Tamilnadu 632014, India*
[3]*School of Computer Science and Engineering (SCOPE), Vellore Institute of Technology, Vellore, Tamilnadu 632014, India*
[4]*School of Information Technology & Engineering (SITE), Vellore Institute of Technology, Vellore, Tamilnadu 632014, India*
[5]*School of Electronics Engineering (SENSE), VIT-AP University, Amaravati, Andhra Pradesh 522237, India*
[6]*School of Mechanical and Automotive Engineering, College of Engineering and Technology, Dilla University, P.O. Box 419, Dilla, Ethiopia*
[7]*Combat Vehicles Research & Development Establishment (CVRDE), Defence Research and Development Organization (DRDO), Ministry of Defence, Government of India, Avadi, Chennai, Tamilnadu 600054, India*

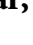Correspondence should be addressed to Senthil Kumaran Selvaraj; senthilkumaranselvaraj82@gmail.com and Addisalem Adefris; addisalem@du.edu.et

Powder bed fusion (PBF) applies to various metallic materials used in the metal printing process of building a wide range of complex parts compared to other AM technologies. PBF process has several variants such as DMLS (direct metal laser sintering), EBM (electron beam melting), SHS (selective heat sintering), SLM (selective laser melting), and SLS (selective laser sintering). For PBF to reach its maximum potential, machine learning (ML) algorithms are used with suitable materials to achieve goals cost-effectively. Various applications of neural networks, including ANNs, CNNs, RNNs, and other popular techniques such as KNN, SVM, and GP were reviewed, and future challenges were discussed. Some special-purpose algorithms were listed as follows: GAN, SeDANN, SCNN, K-means, PCA, etc. This review presents the evolution, current status, challenges, and prospects of these technologies in terms of material, features, process parameters, applications, advantages, disadvantages, etc., to explain their significance and provide an in-depth understanding of the same.

1. Introduction

Powder bed fusion is an additive manufacturing (AM) technique widely used to create products with complex geometries and various materials, especially those with good mechanical properties [1]. PBF is considered the best and most used AM process due to its ability to fabricate metallic or nonmetallic parts with a resolution as small as ±0.02 mm and manufacture homogeneous alloy parts with high strength free-form fabrication with other advantages. Therefore, it is applicable in different sectors, including the medical, automotive, and aerospace industries, because it allows lightweight construction and freedom of design, with fewer parts manufactured locally [2]. Also, it has advantages such as fast prototyping, timesaving manufacturing custom quality designs, and economic benefits such as cost-effectiveness.

Laser powder bed fusion (LPBF) is an ever-growing type of additive manufacturing (AM) technology. This paper studies the

different types of LPBF methods, namely, the direct laser sintering method (DLSM), selective laser melting (SLM), selective heat sintering (SHS), electron beam melting (EBM), and selective laser sintering (SLS). Each of these AM techniques differs fundamentally in its working principle. PBF processes are either full melting or successive sintering processes. Powder material coalesces into solid by heating and direct liquefaction and solidifying powder by intense melting in PBF methods such as SLM, while successive sintering of material is performed to achieve net components in PBF processes such as DMLS. The heating source can be laser and electron beam for high precision fabricated parts.

Moreover, the paper discusses the various process parameters common to all types of AM technology such as laser power, laser spot size, layer thickness, scan speed, and hatch spacing. Optimizing process parameters leads to the efficient part density at lesser lead time. Raw materials are powders classified into aluminum alloys, tool steels, titanium, stainless steel, refractory, and superalloys. The material properties of the fabricated 3D part desired by the end user, such as density, tensile strength, yield strength, elongation at break, hardness value, and roughness value, determine the type and characteristics of the powder used. The powder can have many characteristic aspects that can be varied or changed, such as the grain size or coarseness, diameter, packing density, morphology, and microstructure properties that affect the quality of the fabricated part. This paper reviews process parameters and powder characteristics to minimize the various defects in the LPBF methodology. Defects are undesirable errors due to melt-pool instability, preheat built temperature, and improper process conditions at the in situ and ex situ levels. Some common defects discussed in this review are spherical defects such as porosity, residual stresses at melt-pool, delamination, and geometric defects due to tolerance and balling. The causes and solutions to each defect under various LPBF methods are comprehensively reviewed. Table 1 informs us about some of the most common defects that can be seen in components manufactured using AM techniques, their causes, and their solutions. Integration of ML with AM processes can help us prevent these defects in the very initial phases and even stop manufacturing a defective component as soon as the defect appears with the help of real-time data tracking and decision-making techniques, which can benefit economically as well as avert wastage. By implementing ML, we can optimize input and output characteristics or even predict a component's properties for a given set of input parameters. Thus, ML has immense application in improving AM processes' speed, accuracy, and efficiency and can influence quality outcomes [8].

The current scenario of additive manufacturing has wide applications in aerospace, automotive, prototyping, and medical among many other industries in the 4.0 era [9]. However, it also has limitations in various scenarios such as high residual stress, reproducibility, low porosity, etc. Different types of PBF processes such as DMLS (direct metal laser sintering), EBM (electron beam melting), SHS (selective heat sintering), SLM (selective laser melting), and SLS (selective laser sintering) [10] were studied along with their applications to gain in-depth knowledge of these concepts. Due to the PBF process being step-by-step and working layer-by-layer, there are many conditions and parameters to be kept track of for ideal processing. Since numerous attributes determine the outcome, keeping them manually becomes practically impossible, especially if it has to be done in real time during the procedure. That is where machine learning is employed in this field for smooth, fast, effortless processing.

Today, the use of ML can be seen in many different areas of the AM process [11]. It can help optimize input parameters and output characteristics to get optimal results much faster. Combined with multispectral data used for learning and predicting product quality, it can enhance the printers' efficiency and productivity. It can also enhance build-time estimations, speed up design iterations, optimize cost and weight performance, and enhance our capability to influence part performance by examining the powder and its characteristics. With the introduction of machine learning (ML) such as supervised learning, unsupervised learning, and reinforcement learning algorithms, methods, and techniques depicted in Figure 1 were used to implement tasks such as defect detection, in situ monitoring, real-time process monitoring, quality monitoring, porosity analysis, optimizing process and parameters, parameter selection, prediction of inherent strain, fatigue life, part distortions, and anomalies and parameters like laser power [12–14].

ML can also aid with defects speeding up defect identification and deciding the usability of the component produced via AM. However, one main limitation is that there is a serious lack of technology or application of ML for real-time tracking of the AM process that can simultaneously follow both input parameters and output characteristics observed in every printed layer. This kind of real-time tracking can help keep an eye on the component being manufactured and parallelly keep an eye on the defect formation or development of material properties. Furthermore, with such application, the AM process can be immediately stopped when an undesirable defect such as huge porosity, stress accumulation, or excessive coarsening of grain is formed after a layer of molten powder has coalesced, etc. Stopping the AM process from completing in such cases will help us avoid using more material uselessly when we know the end product will get rejected anyway. It can also save time that will, otherwise, be wasted. All these applications can significantly improve AM process efficiency, productivity, and quality. This real-time tracking can also help maintain stricter and more accurate geometry. In PBF processes, the powders' fluidity, spreading, or flow pattern can significantly influence the defect formation, geometric tolerance, and material characteristics. However, current ML technology for AM applications cannot predict, track, or manipulate such parameters in real time. Scientists are building ML algorithms that can handle huge amounts of data about various input and output parameters, observed and recorded in real time, and simultaneously control these parameters dynamically in real time to achieve required results. These algorithms will be able to do this by being able to predict the powders' flow or spreading. This

TABLE 1: Applications and advantages of different powders.

| Problems	Causes	Solutions	Ref.
Residual stress	The rapid heating and cooling rate resulted in a high-temperature gradient	Postprocess techniques include short peening, heat treatment, age hardening, grinding, and polishing; in-process methods such as controlling scan strategy, feedback control, and mechanical control	[3]
Balling phenomenon	Inadequate input energy results in roughened balls and capillary instability due to the Plateau-Raleigh effect	Lowering the scan speed, increasing laser power, and reducing layer thickness	[4]
Porosity	Gas entrapment in the hollow powders that do not precipitate on solidification. The direct relationship between energy density and cooling time	Scan strategy where the output is scanned twice by the laser at different laser powers; powder flowability and packing density must be optimized	[5]
Delamination	High residual stress-to-yield strength ratio	The temperature gradient at the solid laser freedom must be low	[6]
Geometrical deviations	Alterations in data preprocessing, machine errors, stochastic errors, and deviations in material processing	The compensation cycle algorithm studied by Hartmann et al. concluded to reduce the shrinkage effect	[7]
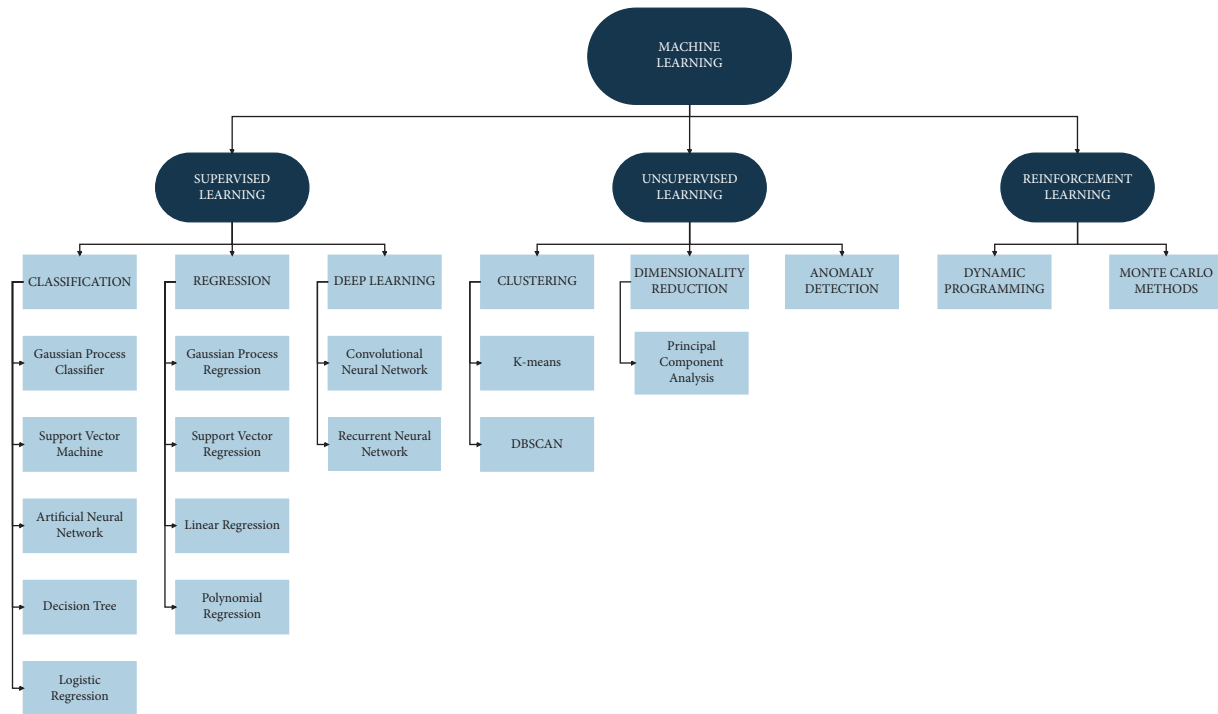
FIGURE 1: Machine learning algorithms are involved in various additive manufacturing processes, including powder bed fusion.

development could also mean faster qualification times and more flexibility for the AM machine user to buy feedstock materials.

Along with the wide applications, machine learning is a recent and developing field. It paves the way for numerous other applications and enhancements concerning the PBF process that are yet to be discovered. For example, architectures/algorithms could be improved upon with ongoing developments and transfer learning. New parameters could also be looked upon, and the accuracy of parameter readings could be improved with the advent of newer technology, such as sensors.

2. Powder Bed Fusion and 3D Printing Technologies

Powder bed fusion is an additive manufacturing technique that enables it to create complex geometries that could not be made/achieved by any other means. Laser powder bed fusion's metal components/parts can incorporate complex designs and achieve the required mechanical properties. Most of the time, reprinting and discarding these parts is observed to eliminate defects. The methods are optimized so that no time and money are wasted in reprinting and discarding these parts. Prototypes and simulations help in achieving the goal.

The PBF process, from the initial stages of data interpretation to the product capability steps, is diagrammatically shown (Figure 2). Data interpretation includes 3D models of all the various formats and defects. The next PBF process proceeds with its process parameters and material requirement. Each and everything is reviewed and then it moves to the next step where product capability is tested, such as its strength, dimension accuracy, and even roughness [4, 15].

Powder bed fusion is an actively used technique in the current day-to-day industry used in producing original and conventional components' sensing, which is available by machine. Manufacturers imply detection of factors like thermal emissions from melt pool; less-known detection is of the emission system for the excited gases which are present as a result of emission of highly excited evaporations can finally conclude that the sensing systems rely on plume monitoring for powder bed fusion [16–19].

Powder bed fusion techniques give out the best results based on factors such as reproductivity and dimensional accuracy in the aspect of part production, and the PBF process uses to fabricate components is a step-by-step procedure repeated layer-by-layer to fabricate a whole component [20–23]. Using a material, various conclusions were drawn out lack of fusion porosity was due to the overlap of the melt pool, where PBF techniques can be used to improve geometric designs, and more complex models of the melt pools dimensionally can be used to predict accuracy [2, 24–27]. As well increased deposition efficiency, characterization, and quantification may result in a more excellent window to identify defects. Powder bed fusion uses methods such as in the process to increase user confidence and encourage further adoption in high-value manufacturing sectors' systems to assess system accuracy and precision [2, 28–31]. The high-value sectors such as biomedical and automobiles have complex geometrical components and different design capabilities and are much more accurate and preferred as the process is layer-by-layer building to achieve such high design complexities [32–37].

One of the forms of AM is powder bed fusion, which has been in the limelight for a few years now because of its unique capabilities of producing 3-D geometries, complex structures,
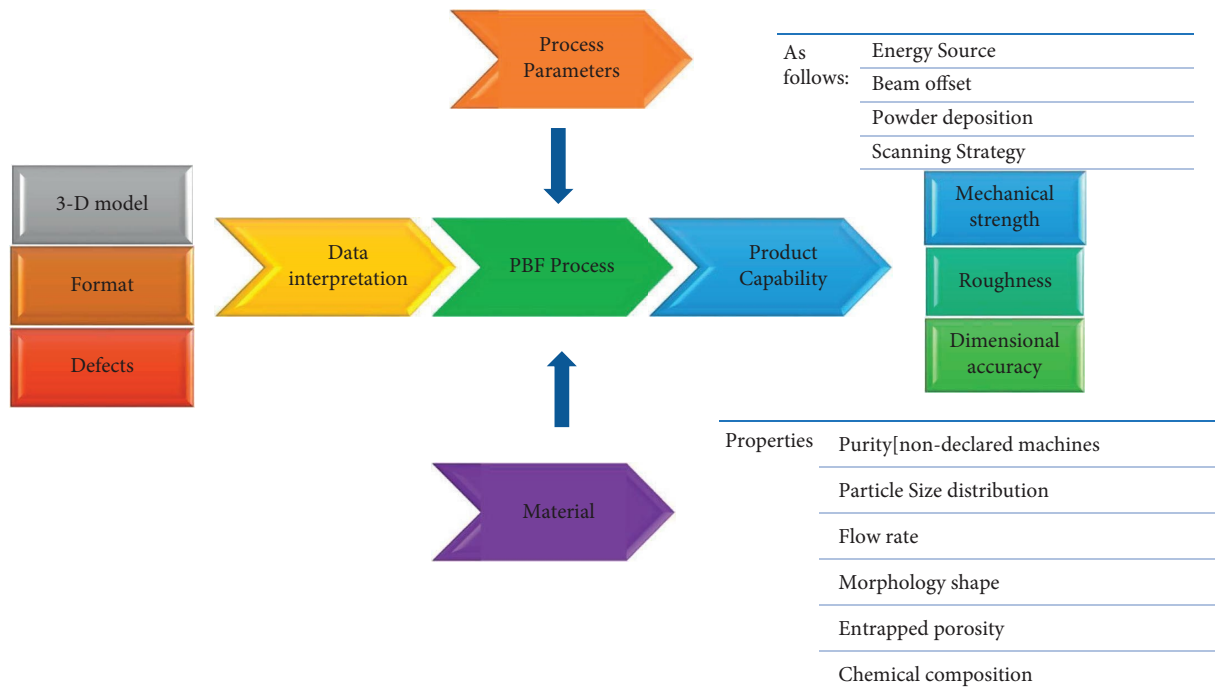
FIGURE 2: PBF processes.

and quality as required, so high-value industries have a keen interest in this process. The layer-by-layer deposition has many advantages as milling, turning, and postprocessing are less involved [38–43].

Powder bed fusion (PBF) is the earliest additive manufacturing process. It is one of the most popular powder-based sintering used for prototyping and in the end-use application in many industries that compete with injection molding and any other polymer manufacturing process [44–46]. These are generally used for low-medium complex parts manufacturing. The laser and electron methods are one of the fastest-growing methods in the industries of methods in DED. They are mostly used for aerospace and biomedical applications due to their properties to make any complex part and excellent material properties. This is a layer-by-layer method, improved build quality, and comparative reduction in cost. The future of this method is quite bright in various fields such as Aerospace Component Manufacturing For Complicated Components and Medical and Industrial Applications [47–49]. One study highlighted this by investigating the dental implants manufactured by the PBF method compared to other conventional methods. The study particularly examined the geometric and dimensional accuracy of the manufactured parts. An approximate increase of around 20% was seen in the PBF samples [50].

3. Types of PBF Processes

Figure 3 explains the various types of processes based on their energy sources. Selective heat sintering comes under thermally fused, selective laser sintering comes under laser fused, and electron beam melting comes under electron beam fused.

3.1. Direct Metal Laser Sintering.
Direct Metal Laser Sintering (DMLS) is an additive manufacturing methodology in which metal powder such as Inconel 625, cobalt chrome, and stainless steel is used to generate a solid three-dimensional model by sintering [1]. The process of joining two entities into one compound by heating and fusing, without melting, is called sintering. The recent advancements in the field of DLMS have found it to be a superior additive manufacturing technology over SLS in reduction of part porosity, manufacturing reliability, postprocessing, and processing time. The DMLS working process consists of the following parts: laser unit, which uses a CO_2 laser, scan head, fiber that connects the laser unit and the scan head, the building platform for layer-by-layer deposition of metal powder, dispenser platform, recoated blade, and collector platform. Metal powder in the dispenser is released one layer at a time from the dispenser platform to the building platform. The relative heights are placed so that the dispenser platform is above the building platform to enable the recoater blade to move without any obstruction. The recoater arm sweeps the powder from left to right motion, and the excess powder is deposited at the collector platform. An inert gas such as argon or neon controls the atmosphere in the chamber construction [2, 9].

In contrast to SLM, the DLMS processes the fabricated parts are generated at 95% density. Thus, it cancels the required successive sintering of the produced parts [2]. In the DMLS process, each layer of powder does not undergo melting and solidification with successive layers, but each layer is heated to a point below the recrystallization temperature, allowing each to fuse with the next one without achieving the melting of the substrate. This is completely different from AM techniques such as SLM as it involves
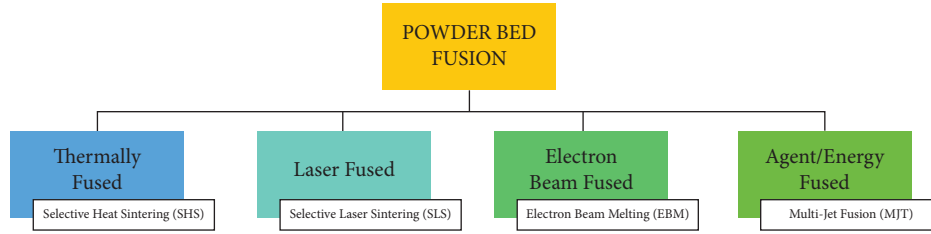
FIGURE 3: Powder bed fusion types based on energy sources.

melting, welding, and solidifying each successive layer. In such a process, the temperature will cross the recrystallization temperature and reach well up to the melting point. In DMLS, the metal powder deployed does not contain fluxing agent or binder and is sintered using a high-power CO_2 laser at 20 to 40 μm layers. The energy absorbed by the metal powder material is measured as absorbance. It is a ratio between the energy flux absorbed by powder matter to the energy flux irradiated by the laser source.

Absorbance can be increased by multiple laser beam reflections, implying a higher optical penetration depth. Apart from absorbance, another important physical phenomenon is the balling effect. Riza et al. found that using a low-power laser resulted in undercooling of the sintered powder, thus forming coarsened balls. Moreover, the balling effect was observed at higher scan speeds along with large-diameter powder balls (~10 μm) [10]. This unwanted phenomenon could be avoided by increasing the volumetric density of energy at the input. The main parameters in DSLM include laser scan speed, hatch spacing, layer thickness, and laser power. The relationship between energy density with the four parameters is given by

$$E = \frac{P}{Vhd},$$ (1)

where $E =>$ energy density (J/mm$\hat{3}$), $P =>$ laser power (W), $V =>$ laser scan speed (mm/s), $h =>$ hatch distance (mm), $d =>$ layer thickness of the powder bed (mm).

The surface roughness depended on the four parameters' laser power and scan speed. Higher laser power and lower scan speed meant more surface roughness. However, it does not depend on the energy density [17].

Upon studying the factors that affect overhanging structures Yap et al., found that higher hatch distance values intensify distortion and accelerate the separation of the part material. Thus, an optimal hatch distance of 0.5 mm was obtained [12]. It was also concluded that laser scan speed does not significantly affect the heat flux in the powder material but reduces the total laser heating time [12]. The scan speed, however, determines the growth of the microstructure. A higher scan speed indicated the presence of small spheroidal balls, giving rise to the balling phenomena [9]. A lower scan speed indicated interagglomerated sintering necks resulting in surface roughness [15]. The layer thickness is a significant process parameter in final surface quality. Decreasing the layer thickness gives a greater surface quality as the spheroidal balls become fully densified. An optimal range for layer

thickness is 0.15–0.25 mm, and flat surfaces were obtained in the preheated tracks [4, 9].

The laser sintering process has four stages. In the first stage, powder atoms from two different surfaces make initial contact. Due to the high surface energy of the particles at contact, necking is formed at a slow growth rate. The particles coalesce, and grain boundary size increases while the surface area decreases. Finally, a full merging of the two particles occurs at an infinite time, and the powder is said to be sintered.

The DLMS process is widely used in implants such as joint reconstructions at the medical forefront. The Ti6Al-4V alloy is used as the powder material as it has good biocompatibility, corrosion resistance, and fatigue resistance. Intricate manufacturing applications in scaffolding find DLMS in demand as it can produce materials with fine porous structures and higher density [10, 16].

However, support structures are required during the sintering process to avoid overhangs. The final fabricated metal part requires postprocessing technologies such as short peening, removal of support structures, and heat treatment [2, 9].

3.2. Electron Beam Melting. Electron beam melting (EBM) is an additive manufacturing methodology often considered rapid prototyping (RP) (Figure 4). EBM uses a high-power electron beam source, unlike the other AM processes, which deploy a laser beam as a heat source for melting and fusing the metal powder. Developed by ARCAM AB, EBM machines have biomedical, automotive, and aerospace applications. A typical EBM machine consists of the following components: a filament made of tungsten, a grid cup for directing the electrons to the anode, anode plates connected to the positive end of the DC voltage supply, focus and deflection coils to adjust the position, and determine the diameter of the beam. The sliced data from the CAD file is differentiated into contours and squares. During the part fabrication, contours are boundaries forming the geometry, which behave as an interface between the metallic powder and part. Squares are the regions formed between the set contours [25]. The build table is placed in an inert vacuum chamber with helium or argon (~10^{-2}-10^{-3} Pa) [29]. The reason is to maintain the integrity of the electron beam, yield high tensile strength, remove any impurities, and maximize the density of the fabricated part. The built platform is initially preheated to a temperature ranging from ~500 to 700°C [27]. Powder materials such as titanium, cobalt chrome, 316 L steel, maraging steel, and Inconel 718 are used as they can conduct electric charge having a particle size ranging between 45 and 100 microns. Electron beam melting
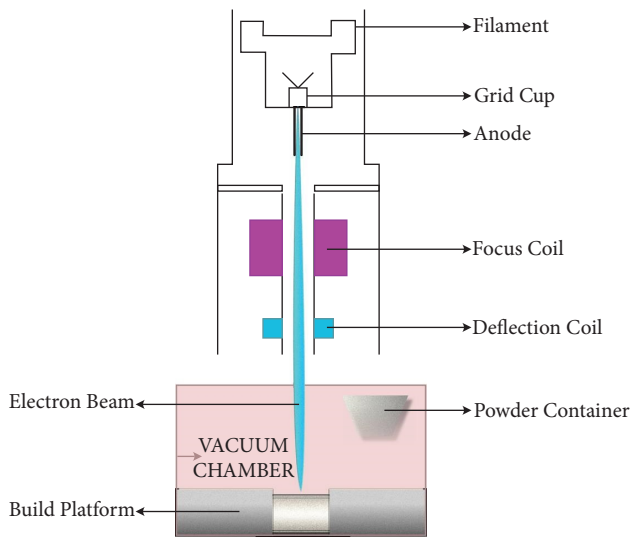
FIGURE 4: EBM processes.

process parameters are classified into scanning parameters such as scan speed and line offset and beam parameters such as beam current and accelerating voltage. The amount of energy incident by the beam on a powder bed is termed energy density. This occurs due to an elastic or inelastic collision of electrons with the material atoms. The significant interactions between the accelerated electrons with the substrates are scattering, backscattering (energy loss), and transmission (energy penetration) [19]. Silvestri et al. found that the backscattering coefficient was directly dependent on beam intensity.

Moreover, the scattering value depends on the target substrate's depth [19]. Surface roughness increased with the decrease in scan speed and beam current. A linear speed calculated as the ratio between beam intensity and scan speed was found to increase with the temperature rise. Scan speed was a deciding parameter in the thermal diffusion time as melt pool temperature was higher at a shorter duration of scan speed. This implies that surface roughness decreases with an increase in temperature. Line offset, the distance between hatch lines was observed to influence material hardness, i.e., with a decrease in a line offset, energy density was higher, leading to rougher microstructures [20]. While studying the surface roughness of inclined parts, Dolimont et al. found that the underside had a lower value for surface roughness than the upper side [18]. Ding et al. studied the correlation between process parameters and melt pool geometry for a single bead experiment at various preheating temperatures, beam powers, and scan speeds. It was deduced that as the line energy (beam power and scan speed) increased, the width and depth of the melt pool strictly increased in accordance with Rosenthal's model for welding [28].

The advantages of EBM type additive manufacturing are mainly the following: reduction in lead time, residual stress reduced due to high process temperature, and the inert gas providing an oxidation-reduction environment. Large-scale industrial production of light switches was developed by an Italian company, BTicino, where EBM technology was used by injection molding [2]. Conformal

cooling channels in cobalt chromium alloys with anti-corrosion and high abrasive resistance were deployed to conduct uniform cooling of the molded part [23, 24]. The fabricated tool displayed 43 HRC Rockwell hardness, yielding 600 MPa, and tensile strength of 900 MPa. The total lead time was effectively one week.

3.3. Selective Laser Melting. Selective laser melting is a type of additive manufacturing process in which a powder bed is melted and layers fused at a high-power laser beam. The setup for the SLM process is similar to DLSM, the difference being the sintering of powder (coalesces without being converted into liquid) instead of melting. The part fabrication begins with slicing CAD file data into layers, and layer thickness ranges from 20 to 100 μm. Each slice is selectively fused using support structures if needed. The final three-dimensional part has up to 99.98% part density as the laser spot size ranges from 20 to 30 μm, creating a melt pool smaller than the EBM process. However, this increases the depth and surface tension of particles around the melt pool, giving rise to more defects in SLM than in EBM. Therefore, a skin-core strategy is used here [30]. The part to be fabricated is classified into an inner core and an outer core forming the skin. The process parameters and focus diameters are distinct in these separate areas. The inner core is manufactured with a beam diameter of 1000 μm and higher laser power (1000 W), subsequently obtaining a higher value of process-relatedbuild-up rate. However, the outer skin is fabricated using a smaller laser beam diameter of 200 μm, focusing on the precision and surface finish of the part.

One of the key undesirable effects of SLM production is residual stress. The direct cause of residual stresses is the varying fluctuations in thermal energy resulting in the crack formation of the fabricated part. Mugwagwa et al., found that upon heat treatment of SLM parts at a range between 600 and 700°C for one hour, the residual stress was reduced by 70% [37]. A recent study by Yasa et al. addresses a newfound scanning strategy termed "sectorial scanning," significantly reducing residual stresses. This method consolidates the various layers into square grids, and adjacent grids are scanned perpendicular to each other [36]. However, ceramic powders show properties of high melting point and low thermal conductivity, resulting in a significantly high thermal gradient during the process. This could be fixed by mixing a eutectic mixture of ammonia and zirconia to reduce the melting temperature to 1860°C [34]. Dross formation is another undesirable formation in low melting metals such as aluminum and tin. In the SLM process, the dross formation was found to reduce in a 30 μm layer thickness compared to 50 μm demonstrating higher strength and lower elongation of the fabricated part [31]. Porosities are spherical defects that occur when gas between powder particles dissolves into the molten pool due to the low packing density of metal powders. Balling effect is an undesirable phenomenon in the SLM process; it occurs when the molten powder does not wet the primary substrate due to surface tension [32]. This increases the surface roughness

and decreases the density of the produced part. Yadroitsev et al. study has concluded that a scan speed of 1 mm/s and laser power of 10 W produced no balling effect as the scan track is widened due to heat conduction, similar to the shrinkage effect [33].

Moreover, in a combination of high scan speed and high laser power, the balling phenomenon does not occur as rapid melt pool solidification occurs behind the laser spot. In a study by Özel et al., increasing the scan velocities tends to decrease the grain sizes in both 67° and 90° rotation strategies. Increasing hatch distance tends to reduce the grain average grain diameters in the case of 90° rotation and is not significant at 67° [35].

SLM materials such as 316 L stainless steel are widely used in the medical industry to develop body implants. Tubular bone, orthodontic products, and mandibular canal segment are a few examples of gradient porosity and stainless steel's strength [32]. Inox 904 L steel produces conformal cooling channels as the wall thickness is about $100\,\mu$m. Other applications include microtooling of steel X110CrMoV Al 8-2, and this metal was produced with high hardness and fine structure simultaneously.

3.4. Selective Laser Sintering. Powder bed fusion is an additive manufacturing process. This can spawn products and make them with precision/accurately. This technique of 3d printing enables the manufacture of complex geometrical components with heat sources, like laser/electron beam, which would fuse the particles of the layer above the layer and finally becomes a solid component. This process substantially gives the manufactures the freedom to design through PBF. It uses a laser to sinter the powdered material layer-by-layer to form a solid material. The product is then brushed to remove the extra or loose powder. The material used in this process SLS is polyamides (basically nylons), alumite (a mixture of polyamide blended with gray aluminum), and rubber-like material. Each material has specific properties, like nylons are strong and flexible, making it one of the best materials for manufacturing springs, brackets, and snap. Designers also consider the possibility of cracking and shrinkage. Sometimes CO_2 laser beam is used. In contrast to DMLS, which can only be used to manufacture parts made of metals, the SLS process can also produce parts made of nonmetals such as composites and polymers. This is one of the main differences between DMLS and SLS.

3.5. Selective Heat Sintering. The SHS process uses a heated thermal head for sintering plastic powders, which get fused due to the heated head as it is touched and moves on the STL model slides. Generally, this process is used to manufacture structural parts, mostly prototypes (concept-based). Selective heat sintering (SHS) process plastic powder particles fuse by a heated head. The heated head touches the powder and moves based on the sliced STL model. This method is used to manufacture structural parts and conceptual prototypes, usually made using polymer or plastic materials. Figure 5 shows the schematics of SHS.
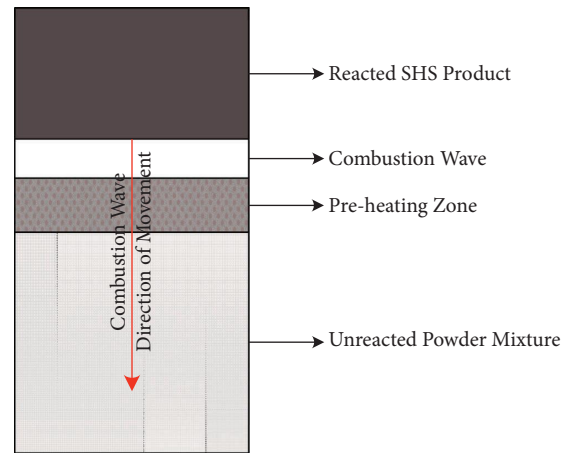

FIGURE 5: Schematic representation of SHS processes.

4. Application of ML in Powder Bed Fusion

Powder bed fusion is an additive manufacturing methodology used to manufacture three-dimensional metallic objects or parts per requirement, i.e., 3D printing of metallic equipment in short. This procedure is carried out by first dividing the part to be manufactured into layers with the help of computer-aided design (CAD) software that gives a model to be followed while constructing. Then, the manufacturing procedure is carried out layer-by-layer sequentially by the spreading of the metallic constituent powder on top of the previous layer, which is then subjected to a moderate amount of heat, usually with the help of a laser power source resulting in their consolidation to form a solid structured layer. For this layer construction, specific parameters must be considered and monitored throughout to ensure that the procedure is carried out in the desired manner and produces the expected outcome, i.e., a flawless part. The production of a flawless part is an entirely ideal situation and is not practically possible. However, the procedure can be worked upon by continuous monitoring to achieve an almost ideal outcome. The manufacturing procedure consists of several parameters that directly affect the outcome, which must be set and kept at specific value ranges throughout the optimal product. This is where machine learning comes into play.

Machine learning is a developing subsection of Artificial Intelligence currently being used in several application areas. It involves a machine trying to learn, as the name suggests, to perform tasks without any explicit programming relating to that specific task. Initially, the machine is passed some inputs and their known correct outputs with the aim of the machine to come up with a correlation between the two so that when an unknown input is passed onto it, it can come up with the output. This particular feature could be twisted to benefit many scenarios in the industry, one of which is in the PBF process. The process consists of specific parameters that a trained machine learning model can monitor. The model is first passed on some particular example readings that resulted in a successfully manufactured product through which it can establish a cooperative relationship between the

parameters and the outcome for an optimal workflow. After being trained on these examples, the model is employed to monitor these parameters and report or change them if it predicts a failed outcome based on the values of the parameters captured then. This particular feature of in situ observation makes the application of machine learning unique and incredibly helpful, as this can help stop the procedure in between if it leads to the manufacturing of a failed product, thus saving a lot of time and resources [51].

There are numerous application areas of machine learning in the field of PBF. Machine learning consists of various algorithms depending on the desired functionality. Some of the algorithms used in this process are K-nearest-neighbors [52], support vector machines [52–55], K-means clustering [56], principal component analysis [57, 58], polynomial regression [59], and Gaussian process regression [58, 60]. These algorithms cover both the supervised and unsupervised learning domains of machine learning.

Supervised learning involves learning the trend between the input and the output to predict the outcome of custom-supplied input accordingly. Thus, the data given to the model for training consists of the parameter values and the target values, i.e., whether the product was successful or not for that particular set of parameter values. These models then come in handy for in situ observation of the procedure.

Unsupervised learning does not involve anything with the output or target values. It aims to separate or cluster the data according to suitability or similarity. Therefore, the data provided to the model does not consist of target values but only of parameter values. These algorithms come in handy when dealing with high-dimensional data, say if the number of parameters under consideration is huge, as the PBF process consists of numerous parameters that affect the quality of the outcome. In this particular scenario, it is hard for supervised algorithms to operate on this data as the complexity and amount of computation are severely high. Thus, unsupervised algorithms, particularly dimensionality reduction algorithms such as the PCA, convert the high dimensional data supplied into a low dimensional data space by either removal of insignificant parameters or simplifying the correlation between numerous parameters.

The parameters described above are basically process parameters or settings based on which the product quality is decided. Those parameters include laser power, scanning speed, beam diameter, melt pool size, and layer angles. All these various algorithms coupled with these numerous parameters to be considered lead to several possibilities where machine learning may be applied in the process and hence serves useful.

In some cases, the complexity of computations becomes high, resulting in the inability of statistical machine learning algorithms to operate effectively. This paves the way for deep learning. Deep learning is a subsection of machine learning, particularly dealing with neural networks, an artificial mimic of the biological brain consisting of a model of a network of interconnected neurons. These neurons communicate with each other and map complex relations between the input and output space, which simple statistical algorithms might be ineffective.

A wide variety of networks exist in this particular domain as well, some of which are artificial neural networks [53, 54, 61–65], convolutional neural networks [53, 54, 64, 66–69], generative adversarial networks [62], spectral convolutional neural networks [70], and sequential decision analysis neural networks [71]. Again, these specialize in different requirements, as seen in the case of statistical algorithms. Thus, this leads to another area of application of machine learning in this field. Algorithms such as the IT2 fuzzy TOPSIS model, vector evaluation genetic algorithm (VEGA), evolutionary algorithms (EAs), and multiobjective evolutionary algorithms (MOEAs) can help in monitoring pBF input parameters in real-time and dynamically controlling them by varying the input values of the most influential input parameters for the elimination of errors and defects, and development of particular properties without compromising on other properties. This ML algorithm application can help reduce uncertainties, errors, and defects during production [69, 72].

The PBF process has numerous stages, from product design development to manufacturing and postprocessing, where ML implementation can be performed. The various stages include the digital phase, where the geometric and material design of the product is decided, and ML algorithms can be integrated into this process to help us in predicting the design or process parameters we need to consider to get a desirable product; in the stage of file preparation we worry about the LPBF part orientation, position, and arrangement on the build platform, all of which can have significant effects on the processing speed, process stability, and part properties. They can also affect the build cost, time, and quality. To improve machine utilization and decrease cost, it is more efficient to pack as many parts as possible in the building envelope. In addition, support structures may also be needed to fix the part onto the build platform and to support overhanging structures.

Furthermore, they are also needed for heat dissipation to avoid residual stresses. However, it is needed to minimize the volume of necessary support structures as they lead to additional material cost, prolong the build time and require postprocess removal. Alternative build orientations are generated efficiently using a nonsupervised ML method and K-means clustering with Davies-Bouldin criterion cluster measuring. Thus, optimizing parameters involved in file preparation; then comes the manufacturing and monitoring phase, where ML techniques can be used to optimize input parameters for the PBF process, monitor these parameters in real time, and dynamically manipulate their values to avoid the formation of defects or uncertainties; and finally, the postprocessing and quality control phases where ML methods can be implemented to automate and improve the efficiency of quality checking of the products produced and also optimize postprocessing input parameters for getting good quality products [73]. ML algorithms can also be implemented to learn from the monitoring and quality checking phases to train themselves to better optimize input parameters for manufacturing and postprocessing.

Applications of machine learning in powder bed fusion include in situ melt pool monitoring, in situ parameter monitoring, in situ defect detection, dimensionality reduction of data, clustering of data points based on parameter values, optimizing parameter values for an optimal outcome, maintaining uniform print quality in all printers, prediction of product density, and prediction of fatigue life. As can be seen, machine learning has a huge number of applications in each of the mentioned areas, along with great scope for future enhancements.

5. Discussion

Figure 6 shows the summary of all the parameters concerning the LPBF process, both in situ and ex situ, describing all the various parameters in PBF. There are three parameters such as process, signature, and product quality. So, under process parameter space, there are 2 subdivisions, namely, controllable and predefined. Next comes the signature parameter space with three subdivisions such as melt pool, track, and layer. Regarding product quality parameter space, there are three subdivisions such as geometric, physical, and mechanical.

Common process parameters in LPBF methods such as DLSM, EBM, SHS, SLS, and SLM include laser scan speed, hatch spacing, laser power source, layer thickness, bed temperature, and scan strategy. The dimensional tolerances which border secondary stresses in part formation are mainly affected by the scanning angle, overhang ratio, and curvature. The relationship between overhang length (L), build angle (s), and thickness of powder layer (t) is given by: $L = t * \tan(s)$ [42]. As the build angle increases, the overhanging surface smoothness increases. In the working chamber, an inert environment is necessary for powder bed fusion as the fabricated part does not come in contact with reactive gases in the atmosphere such as oxygen, nitrogen, and carbon dioxide to produce contaminants. Renishaw's AM250 is an AM machine that deploys a unique approach to maintaining inert gas. First, present gases and humidity within the chamber are removed by forming a vacuum. Subsequently, the chamber is then charged 600 L of pure argon. The atmosphere levels are set at <1000 ppm (0.1% Oxygen), and it deploys gas feed at rates as low as <30 L/hr [74]. Residual stresses caused by rapid changes in temperature gradient can be decreased by postprocessing techniques such as shot peening, heat treatment, age hardening, grinding, and polishing.

Low laser power causes a low cooling rate and lesser formation of liquid, giving rise to coarsened balls. The high scan speed of the laser beam induced melt splashes, causing an agglomeration of the powdered balls. Therefore, the balling effect can be avoided by lowering the scan speed, increasing laser power and reducing layer thickness. Porosities in part fabrication are of two types such as keyhole and contour. Keyhole porosities happen when gas bubbles are trapped due to improper melting/sintering. Contour porosities occur due to substantial differences between hatch and contour tracks [41]. In LBPF, the temperature gradient is largest in the layer build direction (Z direction) as the

cooling occurs more towards the base substrate via conduction and less towards the ambient at the top layer. The production time decreases as the number of lasers increases due to an increase in the build rate per layer.

Increase in the number of lasers increases average powder bed temperature and more area of Heat Affected Zone, which reduces temperature gradient and cooling rate. The peak melt pool temperature value was independent of the scan strategy, and several lasers were used per layer [43]. LPBF in medical field applications seeks material characteristics such as resistance to corrosion, biocompatibility, shear strength, positive elastic modulus, density, and osseointegration. Ti-6AL-4V alloy is, therefore, excellent for surgical and implant applications. Powder morphology, such as particle size distribution, and shape characteristics of individual particles, make for an important parameter in the preprocessing stage. This powder morphology is critical in determining the powder bed's optical penetration depth, thermal conductivity and packing density. Optical penetration leads to the formation of a melt pool. It is defined as the depth at which the radiation intensity inside the material falls to 1/e of the original value. The melt pool's size and cross-section heavily depend on the powder bed's thermal conductivity. A higher densely packed powder bed leads to better ultimate tensile strength [44]. The tensile residual stress developed during the manufacturing process can be minimized by shot peening. It was obtained that anisotropy in the residual stress fields can be controlled by altering the laser pattern of the print, island scan methods, and rotating patterns to reduce anisotropy. Thermal diffusivity and thermal conductivity play a major role in correlation to residual stress. Overall, it was found that such thermal properties played a heavier role than material properties, such as ultimate tensile strength and yield strength in the LPBF process [45].

A 3-D finite element analysis (FEA) is generally deployed to allow the prediction of residual stress and distortion in the multilayer build models. All the common sources of failures in additively manufactured components are the unwanted residual stress and distortion. It is observed that the newly deposited layer generally experiences greater tensile stress while the layers beneath them generally experience compressive stress. The residual stress drives the workpiece's mechanical responses [75].

A Dynamic strategy of adaptive meshing has been developed for the laser powder bed fusion (LPBF) process. This process keeps the fine mesh in the melt pool with the steepest gradient while coarse the rest of its mesh. Updating the mesh at each time frame as the heat source moves, its utility and its accuracy of using dynamic adapting meshing for its simulation (thermal) for the LPBF process is used to predict material properties as well the lack of fusion in it or not [76].

The LPBF process parameters are classified into in situ parameters and significant powder characteristics in Figure 7.

One of the greatest advantages of polymer laser sintering is that it does not require any support structures, which means it has design freedom and fewer post-processing efforts are utilized. The ones where there are overhangs
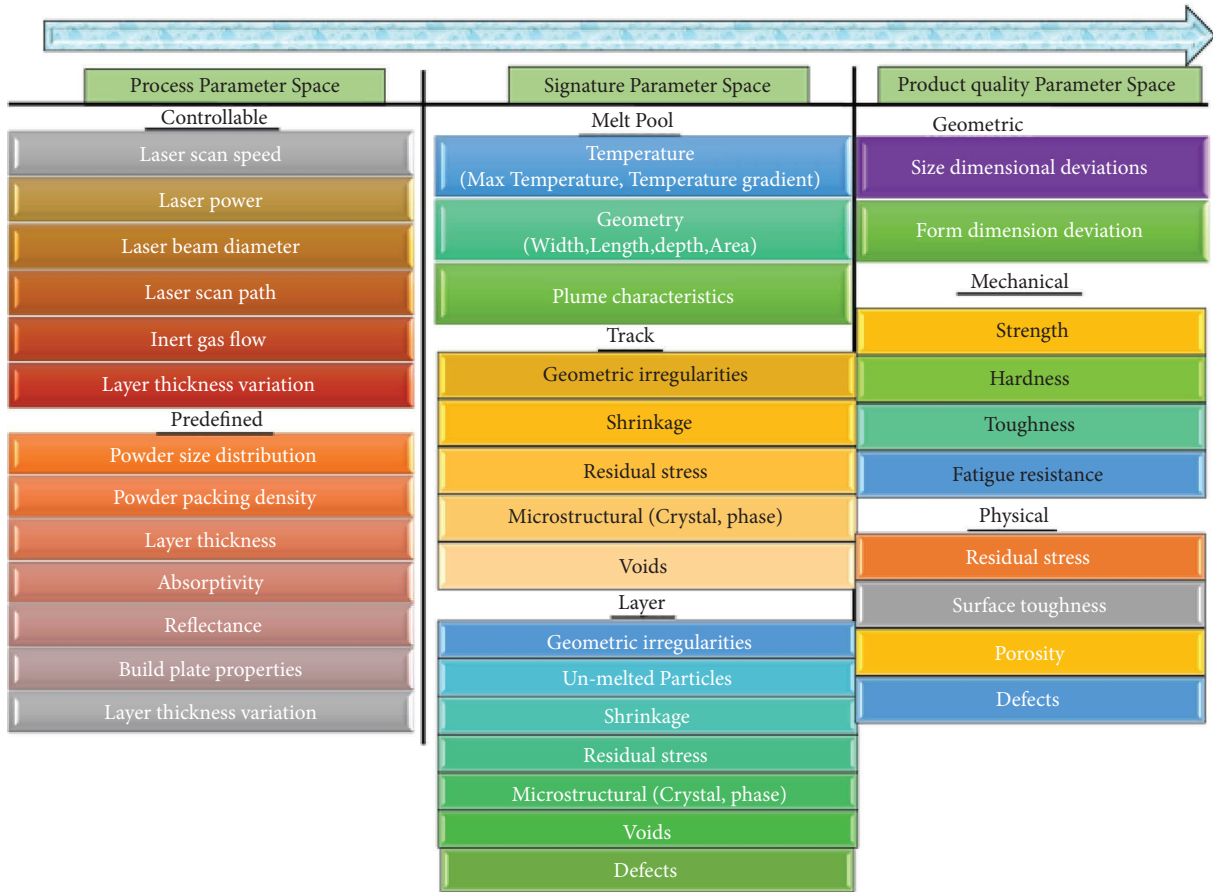
Figure 6: Process parameters of the PBF process.
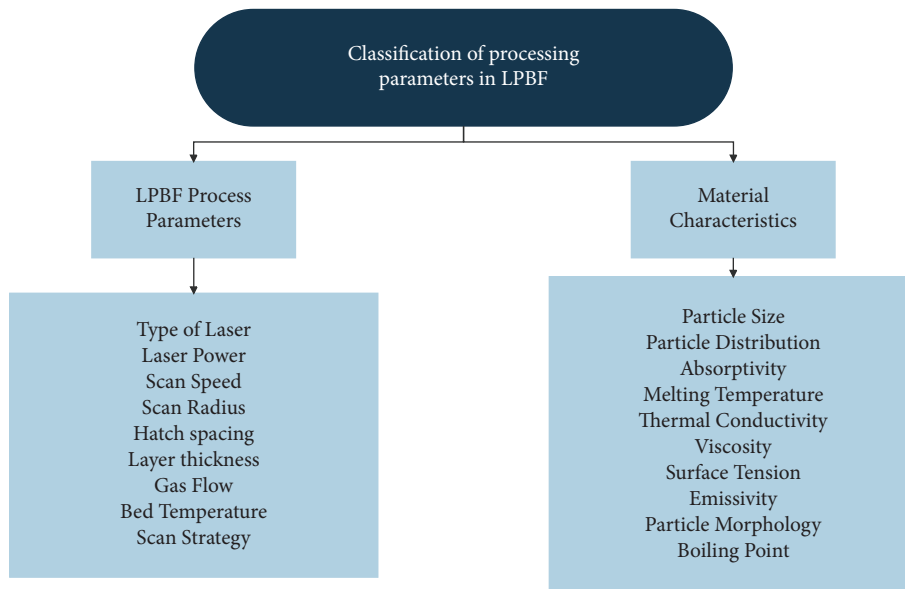
Figure 7: Classification of processing parameters.

used for support must be removed after the completion of the structure or basically when a build is completed/done.

The laser sintering polymer processing can increase the variety of polymers available for usage due to this technique.

However, it was suggested that the concentration must not be only on single layer phenomena but also consider building up bigger/whole structures. All the factors, from monitoring to control, all improvised strategies contribute to

the process that can compete with the conventional manufacturing process [77]. Additive manufacturing to produce an improved version of the useful simulations would significantly reduce wasteful behavior so that it could eliminate the failed parts. It ultimately makes AM a useful, economically feasible, and more widely accepted manufacturing technique [48].

5.1. PostProcessing of LPBF.

The first step in postprocessing is the removal of support structures [39]. In order to avoid collapsing the fabricated part due to its weight, support structures are needed. To optimize and automate this step, ML algorithms can be applied. Regarding the postprocessing of LPBF processed components, handling defects formed and finishing operations to be performed on the component are the most important factors to worry about. Defects that occur in part fabricated by LPBF can be internal or external. Porosities such as spherical, keyhole, or contour are internal defects that affect the part density, thus varying the mechanical and physical properties when measured in different directions. External defects are caused due to rapid melting and solidification, residual stresses, and balling phenomenon resulting in surface roughness and cracking. Internal pores are treated using a hot isostatic press [41].

Moreover, optimizing input parameters for HIPing such as load, dwell time, and pressure to get the best possible component will the least amounts of defects retained, avoid excessive grain coarsening in the case of using certain materials or retainment or enhancement of mechanical properties, can be achieved by the implementation of ML algorithms designed to predict optimal solutions based on extensive trial and error knowledge already accumulated from literature and industry. Doing so can also eliminate human error associated with the trial and error method and aid in faster and more efficient postprocessing. Although the heat treatment helps improve the mechanical properties of the fabricated part, it does not ensure surface smoothness. Nelaturi et al., worked on a refined grain structure protective coating that can be produced in the tiny regions near the surface using drag finishing, vibratory surface finishing, and finished machining processes. Therefore, the fabricated part's microstructural and mechanical characteristics are improved [40]. ML can again help optimize input parameters such as cutting force, use of cutting fluid, depth of cut, and cutting velocity, to get desired results after finishing. Implementing ML can also reduce the chances of human error and help efficiently automize these finishing operations. ML can also be implemented to study, predict, and validate structural and material properties and even correlate material structures of metallic AM and machining properties [78].

5.2. Applications of LPBF Produced Parts.

LPBF finds the most usage of applications in the field of medical, automotive, and aerospace industries. Healthcare systems require parts that are biocompatible along with other characteristics. The production here is low volume. However, it requires rapid prototyping for patients. Parts such as dentures, bone implants, splints, and surgical guides are some examples. Tissue engineering is another good example of the SLS process [46]. LPBF is used in the aerospace industry to produce door clamps for engine front bearing housing. Rolls Royce uses EBM-type AM to produce a titanium front bearing part. Turbine blades, rotor turbines, stators, combustion chambers, fuel nozzles, and air ducts are other components produced using this technique.

Moreover, applications in the field of the automotive industry find use in producing wireless sensors which connect vehicles. Other examples include gear shift knobs, pneumatic and hydraulic systems, prototypes of the headlamp, fuel tanks, gearbox pump impeller, wheel rims, and turbine blades [47]. LPBF is also used as a biomanufacturing technique in the field of tissue engineering, which has enabled the quick fabrication of three-dimensional personalized scaffolds designed to promote tissue regeneration and organs [79]. This is one place where deep learning and ML concepts can help refine and develop better scaffold models that promote enhanced vascularization and better osseointegration. The use of ML can also enable one to predict the appropriate structure and develop various scaffolds with different gradients, mixing different materials in the same scaffold, its properties, and the prediction and correction of their complex architectures [80, 81]. Some commonly used powder materials seen across our review and the properties exhibited by samples made from them with the help of PBF have been listed in Table 2.

5.3. Machine Learning Implementations and Outcomes.

Supervised and unsupervised learning algorithms are used in the powder bed fusion process. Supervised algorithms mainly used in this procedure include linear and logistic regression, support vector machines, Gaussian process regression, and k-nearest neighbors. Linear polynomial regression deals with determining the relationship between an independent and a dependent variable, respectively, or parameters in the case of this process. Using polynomial regression with two models having an average relative error magnitude (AREM) of 23% and 17%, respectively, and the latter being implemented, melt pool variation saw a reduction by a massive 78% by updating the laser power as per the observations of the model [91]. Gaussian process regression has a similar intuition apart from the fact that instead of finding a polynomial relation, it defines a Gaussian distribution that suits the data points. It is used in [57] to determine the relationship between the relative density of the produced part and the laser power and scan speed, giving a prediction error of only 0.3%. It is also used in [74] to assist in the design process of powder bed fusion by giving an idea of the remelted depth of single tracks, which signifies whether the energy used for sintering the powder layers is sufficient or not. K-nearest neighbors (KNN) is another supervised algorithm used both in the case of regression and classification. In [52], KNN is used for regression in which the mean of target values of k-nearest neighbors is taken in the feature space of all parameters, i.e., location, morphology, and size of the defect being the

Table 2: Different powders and their properties.

Powder type	Layer thickness (mm)	Density (g/cm³)	Tensile strength (MPa)	Yield strength (MPa)	E-modulus (GPa)	Elongation at break (%)	Roughness, Ra (μm)	Roughness, Rz (μm)	Hardness (HV)	Ref
AlSi10Mg	0.03–0.1	>2.59	>250	>180	70	>1.0	<20	<80	>80	[82]
Ti-6Al-4V	0.03–0.6	>4.36	>900	>830	110	>10	<20	<80	>310	[83]
IN718	0.03–0.1	>8.07	>940	>750	220	>8	<15	<60	>300	[84]
SS316L	0.03–0.1	—	—	—	—	—	—	—	—	[85]
H13	0.05–0.1	>7.80	>1200	>370	210	>9.0	—	—	—	[86]
IN625		>8.44	>990	>670	170	>35.0	—	—	>30	[87]
ABS-M30	0.18–0.25	1.04	36	—	—	4	—	—	—	[88]
PA 12 (SLS)	0.12	0.95	48	—	—	20	—	—	—	[89]
Polypropylene (PP)	0.12	0.84	32	—	—	529		—	—	[90]

parameters and fatigue life being the target value with a mean squared error value of 1.2736×10^{-3} and R-squared value of 0.96761.

Support vector machine is yet another supervised algorithm that can be used for classification and regression, where it constructs a hyperplane or boundary that contains the maximum average margin value from the associated data points in the feature space [52]. We used an SVM along with a KNN for fatigue life prediction as a function of morphology, location, and defect size with a mean squared error value of 7.0665×10^{-5} and an R-squared value of 0.99418. It is also used in [59] for product density prediction from raw optical signals and can do so with an accuracy of about 93% [55]. We used an SVM to determine whether an abnormality in the produced part is a flaw or a nominal build condition, giving accuracy as high as 85%. As mentioned in [54], SVMs are also used in in situ monitoring of the procedure and reduce defects in the produced part during the process. Unsupervised algorithms include K-means clustering and principal component analysis (PCA), mainly used in the PBF process. K-means clustering involves dividing the data points into "K" clusters, with each point belonging to the cluster with the nearest mean of the cluster to the point itself. In [56], the researchers use K-means clustering for zoning process histories based on thermal data. Principal component analysis is a dimensionality reduction method used to reduce the data's complexity by mapping high feature space data into lower feature space without any significant data loss. The authors of [57, 58] use PCA to reduce the data dimensions for ease of further computation.

Deep learning is another branch of machine learning and artificial intelligence dealing with neural networks that are some of the most advanced algorithms. Neural networks mimic the human nervous system consisting of nodes in place of neurons and the whole network of nodes instead of the nervous system. This interconnection of numerous nodes consisting of innumerable connections in layers helps map complex relations between parameters that statistical machine learning algorithms might fail to perform upon. The neural networks used in the PBF process include artificial neural networks, convolutional neural networks, spectral convolutional neural networks, generative

adversarial networks, and sequential decision analysis neural networks (SeDANN).

Artificial neural networks (ANNs) are the simplest neural networks consisting of layers of nodes interconnected to the preceding and the following layer, respectively, along with an input and an output layer and activation functions to remove linearity [61]. We used ANNs to control and manage the quality of produced parts by identifying the mapping between input process parameters and product quality. Inherent strain prediction is carried out as a function of hatch layer, i.e., angles between different layers of the produced part that gives an idea of product distortions in [63] with the help of an ANN consisting of a single hidden layer and a mean prediction error of 2.78% [64]. We used an ANN consisting of an input layer of 3600 nodes, 9 hidden layers, and an output layer consisting of a single node for prediction of laser power value based on an in situ image of the process, giving an accuracy of about 99%. An ANN with two input nodes, two hidden layers, and four output nodes is used in [65] to map the relation between spreader speeds and layer properties, giving an accuracy of around 96%. Also, as mentioned in [54], ANNs are used for process parameter optimization, in situ observation, control of part geometry, tailoring microstructure and properties, and reducing defects.

Convolutional neural networks (CNNs) is a type of neural network specializing in image-based processing, using the convolution operation between layers. The roughness of produced part from the hyperspectral image is carried out in [66] using a CNN consisting of four convolutional layers, including maxpool layers, a flatten layer, and two dense layers, along with the application of a dropout value of 0.4 to reduce overfitting which yields a final mean absolute error of 2.1 μm [53]. We used CNNs for density prediction from raw optical signals with the architectures of VGG-16 and Alex Net using transfer learning, thus obtaining a training accuracy of 94.88%, validation accuracy of 88.54%, and testing accuracy of 81.24%. The research in [64] also uses CNNs for melt pool monitoring to predict laser power values. In the CNN, three filter sizes (3×3, 5×5, 7×7) and three channel sizes are considered, making the comparison span up to 9 CNNs. In all the CNNs, 4 convolutional layers are used with a stride of 1 and no zero
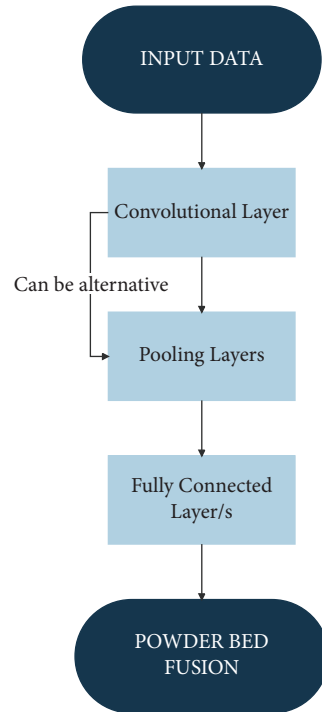
FIGURE 8: Example of a CNN architecture [68].

padding. Maxpool layers follow the first three layers with a stride of 2 and the application of zero padding. The last layer's output shape is adjusted to 1×1 by changing the filter input size. The 3×3 CNN gave lower RMSE values on increasing the channel size. All $\hat{R2}$ values of the 9 CNNs were closer to 1, but the value of the 3×3 CNNs was comparatively closer than others. The 7×7 CNN obtained the best RMSE value with a channel size of $k = 3$. Similarly, [67] uses CNNs for in situ monitoring by taking in situ images as input and predicting the build quality of the produced part with an architecture having four structures consisting of a convolutional layer, rectified linear unit activation, a layer for batch normalization, and an average pooling layer, along with a fully-connected layer, regression layer, input, and output layer. Again, [68] we used CNN for in situ monitoring and thus default detection yielding a mean accuracy of 97.87%. Figure 8 shows a flowchart that depicts a typical example of a CNN architecture, consisting of convolutional and pooling layers in possibly an alternative manner of order, connected in a network for classification with one or more fully-connected layers at the end.

A generative adversarial network (GAN) is a special type of neural network that, if trained adequately, can generate custom images on the required theme. They are used in [62] for generating artificial images of produced parts to train the CNN.

In [71], a sequential decision analysis neural network (SeDANN) is used for monitoring the process to establish reliable part production and reduce quality assessments after obtaining the produced part. It consists of three echelons/levels traversed sequentially by the data for processing. Each echelon plays a role in the processing by giving some significant detail used by the subsequent echelons as input. A SeDANN approach uses elementary statistical attributes that are obtained based on the physical reasoning of the process mechanism, which also facilitates understanding. The first echelon, an ANN, is tasked with predicting laser velocity and power as a function of four variables of the pyrometer signals such as mean, standard deviation, skewness, and kurtosis of the signature of the pyrometer. The second echelon, an ANN, uses these predicted values of power and velocity alongside melt pool image features obtained from rapid video camera images as input and predicts the single-track width.

Additionally, the single-track width standard deviation is obtained by approximating the mean width over three sections of the single-track. The third echelon predicts the percentage continuity as a function of melt pool characteristics and the statistical features predicted in the second echelon. It performed better than all its counterparts, i.e., CNN, LSTM RNNs, SVMs, and KNN, with an average R-squared value of 0.836.

Work in [70] uses a spectral convolutional neural network which is an extension of the convolutional neural networks (CNNs) but can process data of a more complex configuration achieved using irregular convolutions. A

TABLE 3: Additive manufacturing techniques and ML algorithms used, their performance accuracy, and datasets (if available).

Accuracy	ML algorithm used	Additive manufacturing process used	Datasets	Ref
High	SVR, KNN	LPBF	Scanning electron microscopy (SEM) was used for generating 2D defect features. 3D defect features were generated via statistical analysis with the help of high-resolutionX-ray microcomputed tomography; fatigue life data was obtained via high-cycle fatigue tests; using both these features, the dataset was constructed	[92]
High	SVM, SVR, KNN	LPBF or SLM	The data set is established by combining the samples of fatigue life and defect geometry; the dataset is later divided into training and testing data sets	[52]
Not mentioned	CNN	LPBF	From [85], values were acquired in order to decide the laser process parameters, and three-parameter combinations of laser power and scan speed were selected which, includes one having excess energy input (50 W; 40 mm/s) and one with good reproducibility and dense parts (50 W; 75 mm/s), and one with very little energy input (20 W; 75 mm/s) as well as 2 samples were built for these parameter sets for which R_z and the number of frames were later determined	[66]
Not mentioned	SVR	LPBF	Computation of the local thermal histories and the analytical model based on the discrete source approach along with the assumptions and validation studies were utilized from [86], and overall energy input efficiency (η) and the depth-to-width ratio of the volumetric energy source (σ_z/σ_x) were the 2 key parameters for the analytical thermal model which were also described in detail in [86]; moreover, to predict the calibration values in the "full" model, the experimental data that was used in concert with the functions $f_1 = \eta(P, v, w, d)$ and $f_2 = \sigma_z/\sigma_x(P, v, w, d)$ was selected from [86]; the reported width and depth for the "direct" model were also from [86]	[57]
Defect recognition accuracy of 94.18%, 94.32% and 95% from SVM, MLP, and CNN respectively	SVM, MLP, CNN	LPBF	The dataset is extracted from optical data generated involving raw signals; the steps involved are selecting and extracting statistical features, labeling the data, normalization, and then splitting the data into sets	[91]
High accuracy beyond 99% for laser power prediction with FFNN performing better than CNN	FFNN, CNN	LPBF	The melt-pool images used in the dataset were obtained by a metal additive manufacturing equipment monitoring system	[63]
Defect detection validation accuracy of 97.87%	CNN	LPBF	Thermographic off-axis imaging was used to obtain images to form the dataset	[93]

TABLE 3: Continued.

Accuracy	ML algorithm used	Additive manufacturing process used	Datasets	Ref
Spreading prediction accuracy above 96%	Backpropagation neural network	LPBF	Polydispersed digital elevation model simulations are used to obtain data attribute values devoid of noise in contrast to data obtained by physical sensors	[94]
96.80% (mean balanced accuracy) 98.80% (top balanced accuracy) (good)	Deep learning-based neural network (CNN)	LPBF	4,314 RGB color images	[68]
Classification accuracy (83–89%)	SCNN (spectral convolutional neural networks)	SLM	The energy was calculated with the help of the work from [87] Experiment mechanism details are from [88] WPT (details are described in [90]) was used to extract the frequency bands. Feature extraction analysis details where daubechies wavelet was resulted to be the best choice are from [89] All details of the methods: details of the experiment determining the number of layers of SCNN used for classification are from [96] and SCNN through FFT are from [97]	[95]

Table 4: Advantages and disadvantages of the above-stated papers in Table 3.

Advantages	Disadvantages	Ref
(i) In addition to model development and optimization, the statistical analysis helped develop up-to-date mathematical descriptions of powder bed fusion processes	(i) Modeling the sintering process has been difficult as it requires deep information on parameters and properties, especially physical data	[92]
(ii) A combination of two or more methods helps improve the final product quality, for example, FEM (finite element modeling) and ML (machine learning) or statistical analysis with FEM and ML	(ii) Mathematical modeling in combination with FEA (finite element analysis) needs to be improved regarding accuracy and material phase changes in preheating or fabrication of new parts	
(iii) Additional costs are reduced as all the methods use the same type of inputs	(iii) Statistical analysis and ML need a large amount of data to achieve accuracy	
(iv) Experimental and predicted fatigue life are compared and concluded to agree in the case of the SVR model, resulting in a highly accurate regression analysis of SLM processed Ti-6Al-4V alloy		
(v) Using kernel function led to highly efficient regression analysis and non-linear classification. In contrast, the radial basis function was used due to its efficiency and accuracy as compared to models consisting of linear or polynomial kernels	(iv) In terms of structural integrity assessment of metals using additive manufacturing, other parameters such as surface roughness, microstructure, and residual stress should be considered as a collaboration with more testing as well as complex geometrical specimens to generate more practical and definite results for the SVR model	[52]
(vi) KNN and SVR models are highly accurate as they fall under the 1.5 times dispersion line		
(vii) However, compared with KNN, SVM was more accurate in predicting the test set and has good generalization ability		
(viii) Reliable CV was carried out as the result of coefficient of determination corresponds to 0.99 (approx. 1), which is a perfect fit		
(ix) Snapshot hyperspectral imaging combines both spatial and spectral resolution. Therefore, it comes with the benefits of both worlds	(v) Correction/calibration is necessary for snapshot hyperspectral imaging	[66]
(x) At 1070 nm, the direct reflections of laser light could affect the camera; therefore, a short pass filter of 875 nm was used to protect the camera	(vi) Data requirements are high to validate the findings statistically; due to limited samples, the results observed are considered preliminary	
(xi) After the laser exposure in FOV, the saved images are processed to improve data handling	(vii) In comparison with other different sensor technologies, it was found that snapshot hyperspectral imaging has lower temporal as well as spatial resolution when compared to high-speed cameras	
(xii) The camera's orientation was done to collect the maximum number of frames from the scan vectors center	(viii) Also, snapshot hyperspectral imaging has a lower spectral resolution compared to spectrometers	
(xiii) SAX and PCA techniques were used for dimensionality reduction of thermal histories because of various benefits, including statistical, representational, and dimensional	(ix) The configuration formed by the 5×5 patterns called mosaics of Fabry–Pérot filters spread on the CMOS sensor chip is prone to noise induced by nonparallel light beams cross talks, dark currents, chromatic aberration, and vignetting effects of the optical setup	
(xiv) DBSCAN algorithm was used to cluster reduced thermal histories compared to K-means because it is a nonparametric algorithm, and a 5 N-component feature vector is obtained	(x) The training process ends with slight overfitting, as observed during the training	
(xv) Thermal history is considered an appropriate analytical model to obtain process equivalence by finding input energy-efficient strategies. Also, it provides a representation of AM processing of metal that is precise and concise	(xi) Thermal history does not capture occurrences on subsequent layers like lack of fusion defects due to denudation of powder either because of occlusion of the laser beam by spattering or the convection in the vapor	[57]
(xvi) The discrete source analytical method was used to process the scan path's geometric features, such as scan raster properties and vector length in its thermal solution	(xii) The discrete source approach also has limitations, like it does not process the dynamics of melt pool, including sloshing, convection, and waves	
	(xiii) In order to represent processing space completely as thermal history, a few important features are neglected, which could drastically influence the microstructure	

TABLE 4: Continued.

Advantages	Disadvantages	Ref
(xvii) The approach used showed good density prediction performance with 90% accuracy (xviii) The proposed approach is useful in assisting the ML methods to become more accurate and fast (xix) The statistical features-based approach outperformed the deep learning framework in predicting the various density classes (xx) Leave-one-out (LOO) method evaluation showed high inference success rate provided by the proposed CNN	(xiv) It is important to have a sufficiently dense part manufactured to avoid failure during application since porosity/internal pores affect fatigue and mechanical strength as well as causing rupture due to elongation	[91]
(xxi) The proposed model is expected to predict laser power values from melt-pool images to find the difficult position instead of using the AM product tests, which are considered destructive (xxii) The proposed model will be used to check the AM process's reliability, including the accuracy of powder coating, laser irradiation, and laser power values, and to evaluate the defective parts (xxiii) CNN provides highly excellent classification results. It was shown by the confusion matrix that all the delamination defects are classified correctly and are very relevant too (xxiv) The model outperformed with 96.80% of mean balanced accuracy and 98.80% of top balanced accuracy	(xv) The feed-forward neural network showed higher inference accuracy than the proposed network consisting of the 9 CNN's parametric experiment data due to the sensitive reaction of CNN to the variation of the melt-pool images and leading to predicting erroneous laser power(w) values	[63]
(xxv) The proposed model processes the entire image, which is useful in detecting large defect types such as metal splatters. Therefore, considered better for classification as compared to pool monitoring or pixel-wise classification methods (xxvi) The model proposed in this paper is light on computational costs (xxvi) It is a small model, which makes it more specialized and results in highly accurate values	(xvi) CNN cannot detect defects such as pores, unfused powder, balling, and cracks (xvii) The current model only used one geometrical shape and material for training and evaluation	[93]
(xxvii) It does not require extensive data pre-processing (xxviii) The BP-NN with 96% accuracy was used to provide a spreading process map which, when installed in a 3D printer, helps with layer-wise control over spreading defects. It is also used to regress between extensively nonlinear spread layer properties. The model proposed is small, meaning it is more centered to solve a given task and results in higher accuracy (xxix) It requires very less computational costs and resources (xxx) It does not require powerful hardware for training (xxxi) The compilation is fast (xxxii) Also, the temperature difference between delaminated and nondelaminated parts is considered, which is very important for the results. Therefore, heat maps played an important role in the evaluation of the model (xxxiii) The model is not dependent on X-ray imaging and does not require huge data processing	(xviii) The architecture used by the neural network is far too simple and specialized to model the data produced by simulations devoid of noise, thus making it hard for them to generalize to real-time data	[94]

TABLE 4: Continued.

Advantages	Disadvantages	Ref
(xxxiv) The model proposed is small, meaning it is more centered to solve a given task and results in higher accuracy (xxxv) It requires very less computational costs and resources	(xix) Incorrect identification of splatter cases, twenty-two images were classified wrong in which no splatter was present (xx) CNN only has the potential to detect delamination and splatter defects cases, whereas defects such as balling, cracks, unfused powder, and pores remain undetected in the current experimental setup	[68]
(xxxvi) It does not require powerful hardware for training (xxxvii) The compilation is fast (xxxviii) Also, the temperature difference between delaminated and nondelaminated parts is considered, which is very important for the results; therefore, heat maps played an important role in the evaluation of the model (xxxix) The model is not dependent on X-ray imaging and does not require huge data processing (xxxx) AE has many benefits, such as high sensitivity, nondestructive, highly efficient, and cost-effective, over other techniques used in AM processing from past decades for crack initiation and propagation or tracking surface defects (xxxxi) FBG sensor has both high time resolution and sensitivity (xxxxii) SCNN can process irregular data, which can later be optimized using an extern tool during training, which is not possible using traditional convolutional NN (xxxxiii) It was concluded that signals recorded with FBG and processed using SCNN could be highly potential in real-time and in situ monitoring of the AM process	(xxi) Various materials are required to be tested due to variations in their temperature fields, and different geometrical shapes should be used in the training and evaluation of the model, also, to determine the generalizability of the setup towards various types of defects (xxii) In conditions like strong or high-pitch noise backgrounds and weak signals, AE is not very efficient; to overcome these conditions, optical fibers-based AE sensors are used, which are highly sensitive; with the help of ML, AE patterns were extracted even in the presence of noises	[98]

sparse signal representation with a wavelet spectrogram is passed to the neural network using which it can classify the data based on the parameter values calculated from the spectrogram. The model seemed to give an accuracy between 83% and 89%, with the highest accuracy being in the poor-quality part images. It has been discovered that the most common parameters considered in most papers are laser power and scanning speed because they represent the fundamental characteristics of the power source for melting the metal, which is a laser in this case. This assertion is backed by several papers showing prediction and detection accuracies of (>90%) when used with appropriate algorithms. Table 3 gives a list of the ML techniques implemented in various types of PBF methods. Table 4 states the corresponding advantages and disadvantages of the papers stated in Table 3.

6. Summary and Conclusion

Laser powder bed fusion is an additive manufacturing methodology for fabricating metal components. LPBF processes use a high power-density laser beam to selectively fuse a region of powder material; successive layers of a powder material are stacked to build a three-dimensional part. The fused portion of powder material forms a liquid pool, called the melt pool, which solidifies and cools down rapidly [64, 67, 93, 99–101]. The process parameters include laser scan velocity, spot size, hatch spacing, and power. The most common powder used is Ti-6Al-4V alloy. The microstructure properties include relative density, grain size, orientation, and growth direction. The correlation between microstructure properties and possible concerns over the preprocessed three-dimensional component is studied depending on a set of constant process parameters [55, 68, 70, 94, 102]. Melt-pool instability, keyhole effect, irregular microstructure, and subsurface integrity are some of the named concerns. Various reasons and solutions to the part defects are discussed. The postprocessing of LPBF has three stages—support structure removal, heat treatment, and surface smoothening. Each stage is explained to optimize the cost of production. The applications of the LPBF process exponentially grew in the industry 4.0 era. Its usage in automotive, aerospace, medical, and other minor fields is discussed. Additive manufacturing is preferred over subtractive manufacturing for the following reasons: flexibility in design, cost of geometric complexity, need for assemblage, and better lead time. AM can produce any complex geometry as it is a layer-wise fabrication process. However, subtractive manufacturing requires various tooling and fixtures making it harder to cut into depths [56, 60, 65, 69]. Thus, AM has only a few constraints and more degrees of freedom to achieve design functionality. The geometric complexity is directly proportional to the mold cost. Intricate designs require support structures that add to postprocessing. However, compared to traditional injection molding AM does not have an additional cost as there is an absence of tooling and fixturing. This decreases the operational intensity and lead time. Moreover, AM provides dimensional accuracies up to a hundredth of a millimeter.

dimensional tolerance for SLS is ±0.3% (lower limit: ±0.3 mm). AM provides for "single-part assemblies," avoiding the need for integrating different components as in conventional manufacturing.

Further research needs to be done to optimize the process parameters for assessing the manufacturability of LPBF. The defects, including porosities, need further research on correlating them with the existing scan strategies. Process parameters such as laser power and scan speed affect the residual stresses induced in the melt pool, on which the degree of vaporization depends. Moreover, powder morphology and its characteristics play a vital role in microhardness. The formation of overhangs in part fabrication and their dimensional tolerance plays a significant role in postprocessing. One of the factors that affect dimensional tolerance of overhang features is the overhang ratio which is the ratio between self-supported contours and the total value of admissible and inadmissible contours. A direct relationship between borders effect and overhang ratio is found and needs further study to prevent shape deviations of overhangs [98, 103–105]. Melt pool occurs when a laser strikes the powder causing spheroidization and roughness at the track. In order to produce high-quality fabricated parts, melt-pool behavior at various energy parameters (laser power and scanning speed) needs to be studied to reduce the balling effect. The scan strategy rotation is found to determine the size of the powder particle. Desirable powder characteristics, such as high temperature, high tensile strength, and corrosion resistance, must be analyzed at a minimal cost. Applications in tissue engineering are on the rise for SLS type AM. Various biocompatible materials must be researched to obtain medical scaffolds for tissue restoration. Moreover, composite polymeric materials should be investigated for bioactive response to obtain reinforcements such as bioglass, Ag, Cu, and HAp [106–107].

In this era of artificial intelligence, machine learning and deep learning algorithms are used in this PBF process to enhance its quality and reliability. Various algorithms are used, from supervised statistical algorithms such as linear and logistic regression, SVMs, KNNs, and unsupervised algorithms such as K-means clustering to deep learning approaches making use of ANNs, CNNs, GANs, and SeDANNs to carry out tasks such as in situ monitoring of melt-pool signature, process parameters such as laser power and scanning speed, defect detection, quality prediction, and relative density prediction. This monitoring of various factors is carried out in real time, thus reducing the wastage of time and resources to a great extent [108].

Out of these, the most significant algorithm that stands out comparatively regarding metal melting procedures is the ANN. Since it is an artificial mimic of the biological brain, it can capture and process complex relations between parameters effortlessly due to the numerous interconnections between nodes [78, 109–111]. ANNs see applications in several areas in this procedure as described in [54], including process parameter optimization, in situ observation, control of part geometry, tailoring microstructure and properties, and reduced defects. Thus, ANNs are seen to be versatile, thus being helpful in this procedure [112–116]. Most of the

results obtained using this mechanism are also promising, supported by various papers [64, 65] showing the model's accuracy varying in the range of 90's in percentages [109, 117, 118].

However, a few limitations are encountered while applying machine learning in the LPBF process. Statistical analysis and machine learning models, in general, require a huge amount of data conforming to certain standards for effective training and testing, which is hard to gather. Modeling for producing data to train these models is also a complex and difficult procedure due to the huge number of parameters involved. The numerous parameters make it harder for the model to decide on relevant parameters, which might vary based on the material properties [119–126]. The dimensionality reduction models used for reducing the numerous attributes to a few might not generalize well and scrap useful attributes that might turn out relevant on newly encountered data. Even if the data turns out to be sufficient, there is the problem of underfitting and overfitting. A very simple architecture is used in some papers on a smaller biased dataset, thus resulting in a biased model. The other potential problem might be a highly sophisticated architecture specializing in the training data a little too much, thus failing to generalize well with new unseen data. This paves the way for numerous future enhancements that could address these issues, thus improving the model performance significantly than achieved already [127–129].

Abbreviations

SVM:	Support vector machine
ANN:	Artificial neural network
ML:	Machine learning
SVR:	Support vector regression
KNN:	K-nearest neighbor
LPBF:	Laser powder bed fusion
SLM:	Selective laser melting
GridSearchCV:	Grid search with cross-validation
CV:	Cross-validation
MSE:	Mean square error
$R2$:	Coefficient of determination
K:	Number of folds in K-fold CV
AM:	Additive manufacturing
CNN:	Convolutional neural network
MAE:	Mean absolute error
FOV:	Field of view
NN:	Neural networks
AE:	Acoustic emission
SCNN:	Spectral convolutional neural network
SAX:	Symbolic aggregate approximation
PCA:	Principal component analysis
FFNN:	Feed forward neural network
FBG:	Fiber Bragg grating
MLP:	Multilayer perceptron.

Data Availability

All data used to support the findings of the study are included within the article.

Conflicts of Interest

The authors declare that they have no conflicts of interest.

References

[1] T. H. Chio, G. L. Huang, and S. G. Zhou, "Application of direct metal laser sintering to waveguide-based passive microwave components, antennas, and antenna arrays," *Proceedings of the IEEE*, vol. 105, no. 4, pp. 632–644, 2017.

[2] S. Rahmati, "10.12–direct rapid tooling," *Comprehensive materials processing*, vol. 10, pp. 303–344, 2014.

[3] C. Li, Z. Y. Liu, X. Y. Fang, and Y. B. Guo, "Residual stress in metal additive manufacturing," *Procedia CIRP*, vol. 71, pp. 348–353, 2018.

[4] D. Gu and Y. Shen, "Balling phenomena in direct laser sintering of stainless-steel powder: metallurgical mechanisms and control methods," *Materials and Design*, vol. 30, no. 8, pp. 2903–2910, 2009.

[5] A. Du Plessis, I. Yadroitsev, I. Yadroitsava, and S. G. Le Roux, "X-ray microcomputed tomography in additive manufacturing: a review of the current technology and applications," *3D Printing and Additive Manufacturing*, vol. 5, no. 3, pp. 227–247, 2018.

[6] M. Alimardani, E. Toyserkani, J. P. Huissoon, and C. P. Paul, "On the delamination and crack formation in a thin wall fabricated using laser solid freeform fabrication process: an experimental–numerical investigation," *Optics and Lasers in Engineering*, vol. 47, no. 11, pp. 1160–1168, 2009.

[7] C. Hartmann, P. Lechner, B. Himmel, Y. Krieger, T. C. Lueth, and W. Volk, "Compensation for geometrical deviations in additive manufacturing," *Technologies*, vol. 7, no. 4, p. 83, 2019.

[8] P. Gupta, C. Krishna, and R. Rajesh, "Industrial internet of things in intelligent manufacturing a review, approaches, opportunities, open challenges, and future directions," *International Journal of Interactive Design Manufacturing*, 2022.

[9] A. Sharma, A. Chouhan, L. Pavithran, U. Chadha, and S. K. Selvaraj, "Implementation of LSS framework in automotive component manufacturing: a review, current scenario and future directions," *Materials Today Proceedings*, vol. 46, pp. 7815–7824, 2021.

[10] S. H. Riza, S. H. Masood, and C. Wen, "Laser-assisted additive manufacturing for metallic biomedical scaffolds," *Comprehensive Materials Processing*, vol. 10, pp. 285–301, 2014.

[11] U. Chadha, S. K. Selvaraj, A. S. Lamsal et al., "Directed energy deposition via artificial intelligence enabled approaches," *Complexity*, vol. 2022, Article ID 2767371, 32 pages, 2022.

[12] C. Y. Yap, C. K. Chua, Z. L. Dong et al., "Review of selective laser melting: materials and applications," *Applied Physics Reviews*, vol. 2, no. 4, Article ID 041101, 2015.

[13] A. Raj, U. Chadha, and A. Chadha, "Weld quality monitoring via machine learning-enabled approaches," *International Journal Interactive Design Manufacturing*, 2023.

[14] A. Raj, A. Gyaneshwar, and U. Chadha, "Green manufacturing via machine learning enabled approaches," *International Journal of Interactive Design Manufacturing*, 2022.

[15] S. Pal, H. R. Tiyyagura, I. Drstvenšek, and C. S. Kumar, "The effect of post-processing and machining process parameters on properties of stainless steel PH1 product produced by

direct metal laser sintering," *Procedia Engineering*, vol. 149, pp. 359–365, 2016.

[16] A. L. Jardini, M. A. Larosa, C. A. de Carvalho Zavaglia et al., "Customized titanium implant fabricated in additive manufacturing for craniomaxillofacial surgery: this paper discusses the design and fabrication of a metallic implant for the reconstruction of a large cranial defect," *Virtual and Physical Prototyping*, vol. 9, no. 2, pp. 115–125, 2014.

[17] Ö. Poyraz, E. Yasa, G. Akbulut, A. Orhangül, and S. Pilatin, "Investigation of support structures for direct metal laser sintering (DMLS) of IN625 parts," in *Proceedings of the Solid Freeform Fabrication Symposium*, pp. 560–574, Austin, TX, USA, August, 2015.

[18] A. Dolimont, S. Michotte, E. Rivière-Lorphèvre et al., "Influence on surface characteristics of electron beam melting process (EBM) by varying the process parameters," in *Proceedings of the AIP Conference Proceedings*, College Park, MD, USA, October 2017.

[19] A. T. Silvestri, S. Foglia, R. Borrelli, S. Franchitti, C. Pirozzi, and A. Astarita, "Electron beam melting of Ti6Al4V: role of the process parameters under the same energy density," *Journal of Manufacturing Processes*, vol. 60, pp. 162–179, 2020.

[20] A. Mohammad, A. M. Alahmari, M. K. Mohammed, R. K. Renganayagalu, and K. Moiduddin, "Effect of energy input on microstructure and mechanical properties of titanium aluminide alloy fabricated by the additive manufacturing process of electron beam melting," *Materials*, vol. 10, no. 2, p. 211, 2017.

[21] N. Hrabe and T. Quinn, "Effects of processing on microstructure and mechanical properties of a titanium alloy (Ti–6Al–4V) fabricated using electron beam melting (EBM), Part 2: energy input, orientation, and location," *Materials Science and Engineering: A*, vol. 573, pp. 271–277, 2013.

[22] D. Deng, J. Moverare, R. L. Peng, and H. Söderberg, "Microstructure and anisotropic mechanical properties of EBM manufactured Inconel 718 and effects of post heat treatments," *Materials Science and Engineering: A*, vol. 693, pp. 151–163, 2017.

[23] P. Peças, I. Ribeiro, E. Henriques, and A. Raposo, "Additive manufacturing in injection molds—life cycle engineering for technology selection," in *Advanced Applications in Manufacturing Enginering*, pp. 105–139, Woodhead Publishing, Sawston, UK, 2019.

[24] A. Ataee, Y. Li, G. Song, and C. Wen, "Metal scaffolds processed by electron beam melting for biomedical applications," in *Metallic Foam Bone*, pp. 83–110, Woodhead Publishing, Sawston, UK, 2017.

[25] R. Singh, S. Singh, and M. S. J. Hashmi, *Implant Materials And Their Processing Technologies*, Reference Module in Materials Science and Materials Engineering, Elsevie, 2016.

[26] Oshida Y, Bioscience and Bioengineering of Titanium Materials, Elsevier, 2010.

[27] L. C. Zhang, Y. Liu, S. Li, and Y. Hao, "Additive manufacturing of titanium alloys by electron beam melting: a review," *Advanced Engineering Materials*, vol. 20, no. 5, Article ID 1700842, 2018.

[28] X. Ding, Y. Koizumi, D. Wei, and A. Chiba, "Effect of process parameters on melt pool geometry and microstructure development for electron beam melting of IN718: a systematic single bead analysis study," *Additive Manufacturing*, vol. 26, pp. 215–226, 2019.

[29] F. J. Zanner and L. A. Bertram, "Vacuum arc remelting: an overview," *NASA STI/Recon Technical Report N*, vol. 86, Article ID 16417, 1985.

[30] S. Bremen, W. Meiners, and A. Diatlov, "Selective laser melting," *Laser Technik Journal*, vol. 9, no. 2, pp. 33–38, 2012.

[31] A. Charles, A. Elkaseer, L. Thijs, V. Hagenmeyer, and S. Scholz, "Effect of process parameters on the generated surface roughness of down-facing surfaces in selective laser melting," *Applied Sciences*, vol. 9, no. 6, p. 1256, 2019.

[32] B. Zhang, Y. Li, and Q. Bai, "Defect formation mechanisms in selective laser melting: a review," *Chinese Journal of Mechanical Engineering*, vol. 30, no. 3, pp. 515–527, 2017.

[33] I. Yadroitsev, I. Yadroitsava, P. Bertrand, and I. Smurov, "Factor analysis of selective laser melting process parameters and geometrical characteristics of synthesized single tracks," *Rapid Prototyping Journal*, vol. 18, no. 3, pp. 201–208, 2012.

[34] J. P. Kruth, L. Froyen, J. Van Vaerenbergh, P. Mercelis, M. Rombouts, and B. Lauwers, "Selective laser melting of iron-based powder," *Journal of Materials Processing Technology*, vol. 149, no. 1-3, pp. 616–622, 2004.

[35] T. Özel, A. Altay, A. Donmez, and R. Leach, "Surface topography investigations on nickel alloy 625 fabricated via laser powder bed fusion," *International Journal of Advanced Manufacturing Technology*, vol. 94, no. 9-12, pp. 4451–4458, 2018.

[36] E. Yasa, J. Deckers, J. P. Kruth, M. Rombouts, and J. Luyten, "Investigation of sectoral scanning in selective laser melting," in *Proceedings of the Engineering Systems Design and Analysis*, vol. 49187, pp. 695–703, Istanbul, Turkey, January, 2010.

[37] L. Mugwagwa, D. Dimitrov, S. Matope, and I. Yadroitsev, "Influence of process parameters on residual stress related distortions in selective laser melting," *Procedia Manufacturing*, vol. 21, pp. 92–99, 2018.

[38] Y. L. Hu, X. Lin, Y. L. Li et al., "Plastic deformation behavior and dynamic recrystallization of Inconel 625 superalloy fabricated by directed energy deposition," *Materials and Design*, vol. 186, Article ID 108359, 2020.

[39] K. Cooper, P. Steele, B. Cheng, and K. Chou, "Contact-free support structures for part overhangs in powder-bed metal additive manufacturing," *Inventions*, vol. 3, no. 1, 2017.

[40] S. Nelaturi, M. Behandish, A. M. Mirzendehdel, and J. de Kleer, "Automatic support removal for additive manufacturing post processing," *Computer-Aided Design*, vol. 115, pp. 135–146, 2019.

[41] M. Bayat, A. Thanki, S. Mohanty et al., "Keyhole-induced porosities in laser-based powder bed fusion (L-PBF) of Ti6Al4V: high-fidelity modelling and experimental validation," *Additive Manufacturing*, vol. 30, Article ID 100835, 2019.

[42] L. Dowling, J. Kennedy, S. O'Shaughnessy, and D. Trimble, "A review of critical repeatability and reproducibility issues in powder bed fusion," *Materials and Design*, vol. 186, Article ID 108346, 2020.

[43] Renishaw, "Atmosphere-generation," 2020, https://www.renishaw.com/en/inert-atmosphere-generation--31885.

[44] M. Masoomi, S. M. Thompson, and N. Shamsaei, "Laser powder bed fusion of Ti-6Al-4V parts: thermal modeling and mechanical implications," *International Journal of Machine Tools and Manufacture*, vol. 118-119, pp. 73–90, 2017.

[45] A. Mussatto, R. Groarke, A. O'Neill, M. A. Obeidi, Y. Delaure, and D. Brabazon, "Influences of powder morphology and spreading parameters on the powder bed topography uniformity in powder bed fusion metal additive

manufacturing," *Additive Manufacturing*, vol. 38, Article ID 101807, 2021.

[46] A. Kempf and K. Hilgenberg, "Influence of sub-cell structure on the mechanical properties of AlSi10Mg manufactured by laser powder bed fusion," *Materials Science and Engineering: A*, vol. 776, Article ID 138976, 2020.

[47] K. H. Tan, C. K. Chua, K. F. Leong et al., "Selective laser sintering of biocompatible polymers for applications in tissue engineering," *Bio-Medical Materials and Engineering*, vol. 15, no. 1-2, pp. 113–124, 2005.

[48] L. J. Kumar and C. G. Krishnadas Nair, "Current trends of additive manufacturing in the aerospace industry," *Advances in 3D Printing and Additive Manufacturing Technologies*, pp. 39–54, 2016.

[49] M. Gouge and P. Michaleris, "An introduction to additive manufacturing processes and their modelling challenges," in *Thermo-mechanical Modeling of Additive Manufacturing*, pp. 3–18, Butterworth-Heinemann, Oxford, UK, 2018.

[50] Y. Liu, S. L. Sing, R. Xin En Lim, W. Y. Yeong, and B. T. Goh, "Preliminary investigation on the geometric accuracy of 3D printed dental implant using a monkey maxilla incisor model," *International Journal of Bioprinting*, vol. 8, no. 1, pp. 476–573, 2022.

[51] G. K. Sarkon, B. Safaei, M. S. Kenevisi, S. Arman, and Q. Zeeshan, "State-of-the-art review of machine learning applications in additive manufacturing; from design to manufacturing and property control," *Archives of Computational Methods in Engineering*, vol. 29, 2022.

[52] M. Marrey, E. Malekipour, H. El-Mounayri, and E. J. Faierson, "A framework for optimizing process parameters in powder bed fusion (pbf) process using artificial neural network (ann)," *Procedia Manufacturing*, vol. 34, pp. 505–515, 2019.

[53] R. Liu, S. Liu, and X. Zhang, "A physics-informed machine learning model for porosity analysis in laser powder bed fusion additive manufacturing," *International Journal of Advanced Manufacturing Technology*, vol. 113, no. 7-8, pp. 1943–1958, 2021.

[54] A. Gaikwad, F. Imani, H. Yang, E. Reutzel, and P. Rao, "In situ monitoring of thin-wall build quality in laser powder bed fusion using deep learning," *Smart and Sustainable Manufacturing Systems*, vol. 3, no. 1, Article ID 20190027, 2019.

[55] S. P. Donegan, E. J. Schwalbach, and M. A. Groeber, "Zoning additive manufacturing process histories using unsupervised machine learning," *Materials Characterization*, vol. 161, Article ID 110123, 2020.

[56] E. J. Schwalbach, S. P. Donegan, M. G. Chapman, K. J. Chaput, and M. A. Groeber, "A discrete source model of powder bed fusion additive manufacturing thermal history," *Additive Manufacturing*, vol. 25, pp. 485–498, 2019.

[57] A. Gaikwad, B. Giera, G. M. Guss, J. B. Forien, M. J. Matthews, and P. Rao, "Heterogeneous sensing and scientific machine learning for quality assurance in laser powder bed fusion–A single-track study," *Additive Manufacturing*, vol. 36, Article ID 101659, 2020.

[58] L. Li and S. Anand, "Hatch pattern based inherent strain prediction using neural networks for powder bed fusion additive manufacturing," *Journal of Manufacturing Processes*, vol. 56, pp. 1344–1352, 2020.

[59] T. DebRoy, T. Mukherjee, H. L. Wei, J. W. Elmer, and J. O. Milewski, "Metallurgy, mechanistic models and machine learning in metal printing," *Nature Reviews Materials*, vol. 6, pp. 48–68, 2020.

[60] M. Gieseke, C. Noelke, S. Kaierle, V. Wesling, and H. Haferkamp, "Selective laser melting of magnesium and magnesium alloys," in *Magnesium Technology 2013*, pp. 65–68, Springer, Cham, Switzerland, 2013.

[61] S. Srinivasan, B. Swick, and M. A. Groeber, "Laser powder bed fusion parameter selection via machine-learning-augmented process modeling," *Journal of Occupational Medicine*, vol. 72, no. 12, pp. 4393–4403, 2020.

[62] H. Yeung, Z. Yang, and L. Yan, "A meltpool prediction based scan strategy for powder bed fusion additive manufacturing," *Additive Manufacturing*, vol. 35, Article ID 101383, 2020.

[63] O. Kwon, H. G. Kim, W. Kim, G. H. Kim, and K. Kim, "A convolutional neural network for prediction of laser power using melt-pool images in laser powder bed fusion," *IEEE Access*, vol. 8, pp. 23255–23263, 2020.

[64] M. Amini, S. I. Chang, and P. Rao, "A cybermanufacturing and AI framework for laser powder bed fusion (LPBF) additive manufacturing process," *Manufacturing Letters*, vol. 21, pp. 41–44, 2019.

[65] K. Wasmer, C. Kenel, F. Saeidi, C. Leinenbach, and S. A. Shevchik, "In situ and real-time monitoring of powder-bed AM by combining acoustic emission and machine learning," in *Proceedings of the Conference proceedings, Laser in Manufacturing (LiM2017)*, Munich, Germany, June 2017.

[66] X. Zhang, J. Saniie, and A. Heifetz, "Detection of defects in additively manufactured stainless steel 316L with compact infrared camera and machine learning algorithms," *Journal of Occupational Medicine*, vol. 72, no. 12, pp. 4244–4253, 2020.

[67] O. Fergani and K. Eissing, "A machine learning-based digital twin of the manufacturing process: metal powder-bed fusion case," 2020, https://engrxiv.org/preprint/view/878.

[68] L. Meng, "Machine learning and probabilistic design framework for laser powder bed FUSION process," Doctoral dissertation, Purdue University Graduate School, West Lafayette, IN, USA, 2020.

[69] G. Kou, H. Xiao, M. Cao, and L. H. Lee, "Optimal computing budget allocation for the vector evaluated genetic algorithm in multi-objective simulation optimization," *Automatica*, vol. 129, Article ID 109599, 2021.

[70] H. Elwarfalli, D. Papazoglou, D. Erdahl, A. Doll, and J. Speltz, "In Situ process monitoring for laser-powder bed fusion using convolutional neural networks and infrared tomography," in *Proceedings of the 2019 IEEE National Aerospace and Electronics Conference (NAECON)*, pp. 323–327, IEEE, Dayton, OH, USA, July 2019.

[71] Y. Zhu, Z. Wu, W. D. Hartley, J. M. Sietins, C. B. Williams, and H. Z. Yu, "Unraveling pore evolution in post-processing of binder jetting materials: X-ray computed tomography, computer vision, and machine learning," *Additive Manufacturing*, vol. 34, Article ID 101183, 2020.

[72] G. Kou, O. Olgu Akdeniz, H. Dincer, and S. Yuksel, "fintech investments in European banks: a hybrid IT2 fuzzy multi-dimensional decision-making approach," *Financial innovation*, vol. 7, no. 1, p. 39, 2021.

[73] S. L. Sing, C. N. Kuo, C. T. Shih, C. C. Ho, and C. K. Chua, "Perspectives of using machine learning in laser powder bed fusion for metal additive manufacturing," *Virtual and Physical Prototyping*, vol. 16, no. 3, pp. 372–386, 2021.

[74] R. F. Pereira and P. J. Bártolo, "Recent advances in additive biomanufacturing," *Comprehensive Materials Processing*, vol. 10, 2014.

[75] E. R. Denlinger, "Development and numerical verification of a dynamic adaptive mesh coarsening strategy for simulating

laser power bed fusion processes," in *Thermo-Mechanical Modeling of Additive Manufacturing*, pp. 199–213, Butterworth-Heinemann, Oxford, UK, 2018.

[76] C. Vyas, G. Poologasundarampillai, J. Hoyland, and P. Bartolo, "3D printing of bio composites for osteochondral tissue engineering," in *Biomedical Composites*, pp. 261–302, Woodhead Publishing, Sawston, UK, 2017.

[77] S. Sun, M. Brandt, and M. J. L. A. M. Easton, "Powder bed fusion processes: an overview," *Laser Additive Manufacturing*, pp. 55–77, Woodhead Publishing, Sawston, UK, 2017.

[78] X. Gong, D. Zeng, W. Groeneveld-Meijer, and G. Manogharan, "Additive manufacturing: a machine learning model of process-structure-property linkages for machining behavior of Ti-6Al-4V," *Mater Sci Add Manuf*, vol. 1, no. 1, p. 6, 2022.

[79] E. R. Denlinger, M. Gouge, J. Irwin, and P. Michaleris, "Thermomechanical model development and in situ experimental validation of the Laser Powder-Bed Fusion process," *Additive Manufacturing*, vol. 16, pp. 73–80, 2017.

[80] R. Goodridge and S. Ziegelmeier, "Powder bed fusion of polymers," in *Laser Additive Manufacturing*, pp. 181–204, Woodhead Publishing, Sawston, UK, 2017.

[81] S. L. Sing, "Perspectives on additive manufacturing enabled beta-titanium alloys for biomedical applications," *International Journal of Bioprinting*, vol. 8, no. 1, pp. 478–8, 2022.

[82] S. Vock, B. Klöden, A. Kirchner, T. WeiBgarber, and B. Kieback, "Powders for powder bed fusion: a review," *Prog Addit Manuf*, vol. 4, pp. 383–397, 2019.

[83] Stratasys, "Direct Metal Laser Sintering (DMLS)," 2023, https://www.stratasysdirect.com/technologies/direct-metal-laser-sintering.

[84] Matweb, "AISI Type H13 Hot Work Tool Steel," 2022, http://www.matweb.com/search/datasheet_print.aspx?matguid=e30d1d1038164808a85cf7ba6aa87ef7.

[85] Matmatch, "Learn material," 2022, https://matmatch.com/learn/material/inconel-625.

[86] Javelin, "ABS-M30 FDM Plastic," 2023, https://www.javelin-tech.com/3d/stratasys-materials/abs-m30.

[87] H. Christina, "Materials Spotlight: The Properties of Nylon 12," 2022, https://www.cableorganizer.com/learning-center/articles/materials-nylon12.html.

[88] Simplify3d, "Polypropylene," 2020, https://www.simplify3d.com/support/materials-guide/polypropylene/#:%7E:text=Polypropylene%20is%20a%20semi%2Drigid,it%20challenging%20to%203D%20print.

[89] I. Arasu, K. Chockalingam, C. Kailasanathan, and M. Sivabharathy, "Optimization of surface roughness in selective laser sintered stainless steel parts," *International Journal of ChemTech Research*, vol. 6, no. 5, pp. 2993–2999, 2014.

[90] T. D. Ngo, A. Kashani, G. Imbalzano, K. T. Nguyen, and D. Hui, "Additive manufacturing (3D printing): a review of materials, methods, applications and challenges," *Composites Part B: Engineering*, vol. 143, pp. 172–196, 2018.

[91] W. Zouhri, J. Y. Dantan, B. Häfner et al., "Optical process monitoring for laser-powder bed fusion (L-PBF)," *CIRP Journal of Manufacturing Science and Technology*, vol. 31, pp. 607–617, 2020.

[92] I. Baturynska, O. Semeniuta, and K. Martinsen, "Optimization of process parameters for powder bed fusion additive manufacturing by combination of machine learning and finite element method: a conceptual framework," *Procedia CIRP*, vol. 67, pp. 227–232, 2018.

[93] H. Baumgartl, J. Tomas, R. Buettner, and M. Merkel, "A deep learning-based model for defect detection in laser-powder bed fusion using in-situ thermographic monitoring," *Progress in Additive Manufacturing*, vol. 5, no. 3, pp. 277–285, 2020.

[94] P. S. Desai and C. F. Higgs, "Spreading process maps for powder-bed additive manufacturing derived from physics model-based machine learning," *Metals*, vol. 9, no. 11, p. 1176, 2019.

[95] L. Thijs, F. Verhaeghe, T. Craeghs, J. V. Humbeeck, and J. P. Kruth, "A study of the microstructural evolution during selective laser melting of Ti–6Al–4V," *Acta Materialia*, vol. 58, no. 9, pp. 3303–3312, 2010.

[96] P. O'Regan, P. Prickett, R. Setchi, G. Hankins, and N. Jones, "Metal based additive layer manufacturing: variations, correlations and process control," *Procedia Computer Science*, vol. 96, pp. 216–224, 2016.

[97] R. Singh, A. Gupta, O. Tripathi et al., "Powder bed fusion process in additive manufacturing: an overview," *Materials Today Proceedings*, vol. 26, pp. 3058–3070, 2020.

[98] S. Bland and N. T. Aboulkhair, "Reducing porosity in additive manufacturing," *Metal Powder Report*, vol. 70, no. 2, pp. 79–81, 2015.

[99] M. Grasso and B. M. Colosimo, "A statistical learning method for image-based monitoring of the plume signature in laser powder bed fusion," *Robotics and Computer-Integrated Manufacturing*, vol. 57, pp. 103–115, 2019.

[100] B. Yuan, G. M. Guss, A. C. Wilson et al., "Machine-learning-based monitoring of laser powder bed fusion," *Advanced Materials Technologies*, vol. 3, no. 12, Article ID 1800136, 2018.

[101] C. Gobert, E. W. Reutzel, J. Petrich, A. R. Nassar, and S. Phoha, "Application of supervised machine learning for defect detection during metallic powder bed fusion additive manufacturing using high resolution imaging," *Additive Manufacturing*, vol. 21, pp. 517–528, 2018.

[102] K. Wasmer, C. Kenel, C. Leinenbach, and S. A. Shevchik, "In situ and real-time monitoring of powder-bed AM by combining acoustic emission and artificial intelligence," in *Proceedings of the International Conference on Additive Manufacturing in Products and Applications*, pp. 200–209, Springer, Cham, Switzerland, September, 2017.

[103] I. Daubechies, "Ten lectures on wavelets," *Society for industrial and applied mathematics*, 1992.

[104] M. V. Tazebay and A. N. Akansu, "Adaptive subband transforms in time-frequency excisers for DSSS communications systems," *IEEE Transactions on Signal Processing*, vol. 43, no. 11, pp. 2776–2782, 1995.

[105] S. A. Shevchik, C. Kenel, C. Leinenbach, and K. Wasmer, "Acoustic emission for in situ quality monitoring in additive manufacturing using spectral convolutional neural networks," *Additive Manufacturing*, vol. 21, pp. 598–604, 2018.

[106] T. Ghimire, A. Joshi, S. Sen, C. Kapruan, U. Chadha, and S. K. Selvaraj, "Blockchain in additive manufacturing processes: recent trends and its future possibilities," *Materials Today Proceedings*, vol. 50, pp. 2170–2180, 2022.

[107] U. Chadha, A. Abrol, N. P. Vora, A. Tiwari, S. K. Shanker, and S. K. Selvaraj, "Performance evaluation of 3D printing technologies: a review, recent advances, current challenges, and future directions," *Prog Addit Manuf*, vol. 7, no. 5, pp. 853–886, 2022.

[108] R. Sivasubramani, A. Verma, G. Rithvik, U. Chadha, and S. Senthil Kumaran, "Influence on nonhomogeneous microstructure formation and its role on tensile and fatigue performance of duplex stainless steel by a solid-state welding process," *Materials Today Proceedings*, vol. 46, pp. 7284–7296, 2021, 17.

[109] A. Raj, S. Ram Kishore, L. Jose, A. K. Karn, U. Chadha, and S. K. Selvaraj, "A survey of electromagnetic metal casting computation designs, present approaches, future possibilities, and practical issues," *The European Physical Journal Plus*, vol. 136, no. 6, p. 704, 2021.

[110] K. Virmani, C. Deepak, S. Sharma, U. Chadha, and S. K. Selvaraj, "Nanomaterials for automotive outer panel components: a review," *The European Physical Journal Plus*, vol. 136, no. 9, p. 921, 2021.

[111] U. Chadha, S. K. Selvaraj, A. K. Ravinuthala et al., "Bio-inspired techniques in freeze casting: a survey of processes, current advances, and future directions," *International Journal of Polymer Science*, vol. 2022, Article ID 9169046, 22 pages, 2022.

[112] S. K. Selvaraj, A. Raj, R. Rishikesh Mahadevan, U. Chadha, and V. Paramasivam, "A review on machine learning models in injection molding machines," *Advances in Materials Science and Engineering*, vol. 2022, Article ID 1949061, 28 pages, 2022.

[113] S. K. Selvaraj, A. Raj, M. Dharnidharka et al., "A cutting-edge survey of tribological behavior evaluation using artificial and computational intelligence models," *Advances in Materials Science and Engineering*, vol. 2021, Article ID 9529199, 17 pages, 2021.

[114] M. Dharnidharka, U. Chadha, L. M. Dasari, A. Paliwal, Y. Surya, and S. K. Selvaraj, "Optical tomography in additive manufacturing: a review, processes, open problems, and new opportunities," *The European Physical Journal Plus*, vol. 136, no. 11, p. 1133, 2021.

[115] V. Madhavadas, D. Srivastava, U. Chadha et al., "A review on metal additive manufacturing for intricately shaped aerospace components," *CIRP Journal of Manufacturing Science and Technology*, vol. 39, pp. 18–36, 2022.

[116] U. Chadha, S. K. Selvaraj, A. Raj et al., "AI-driven techniques for controlling the metal melting production: a review, processes, enabling technologies, solutions, and research challenges," *Materials Research Express*, vol. 9, no. 7, Article ID 072001, 2022.

[117] S. S. Patel, M. Surjith Shiva, T. Kataray et al., "Trends in tribological behaviour of materials for compressors," *Journal of Physics: Conference Series*, vol. 2272, no. 1, Article ID 012023, 2022.

[118] U. Chadha, S. K. Selvaraj, N. Gunreddy et al., "A survey of machine learning in friction stir welding, including unresolved issues and future research directions," *Material Design and Processing Communications*, vol. 2022, Article ID 2568347, 28 pages, 2022.

[119] V. Carlota, "The Complete Guide to Electron Beam Melting (EBM) in 3D Printing," 2023, https://www.3dnatives.com/en/electron-beam-melting100420174/.

[120] Aniwaa, "Arcam Q20 overview," 2023, https://www.aniwaa.com/product/3d-printers/arcam-q20/.

[121] Slm-solutions, "The makers industrial metal am machines scroll down," 2023, https://www.slm-solutions.com/products-and-solutions/machines/.

[122] L. Meng, B. McWilliams, W. Jarosinski et al., "Machine learning in additive manufacturing: a review," *Journal of Occupational Medicine*, vol. 72, no. 6, pp. 2363–2377, 2020.

[123] H. Bao, S. Wu, Z. Wu, G. Kang, X. Peng, and P. J. Withers, "A machine-learning fatigue life prediction approach of additively manufactured metals," *Engineering Fracture Mechanics*, vol. 242, Article ID 107508, 2021.

[124] N. Gerdes, C. Hoff, J. Hermsdorf, S. Kaierle, and L. Overmeyer, "Snapshot hyperspectral imaging for quality assurance in laser powder bed fusion," *Procedia CIRP*, vol. 94, pp. 25–28, 2020.

[125] L. Scime, D. Siddel, S. Baird, and V. Paquit, "Layer-wise anomaly detection and classification for powder bed additive manufacturing processes: a machine-agnostic algorithm for real-timepixel-wise semantic segmentation," *Additive Manufacturing*, vol. 36, Article ID 101453, 2020.

[126] Q. Liu, H. Wu, M. J. Paul et al., "Machine-learning assisted laser powder bed fusion process optimization for AlSi10Mg: new microstructure description indices and fracture mechanisms," *Acta Materialia*, vol. 201, pp. 316–328, 2020.

[127] M. Mathieu, M. Henaff, and Y. LeCun, "Fast training of convolutional networks through FFTS: international conference on learning representations (ICLR2014), CBLS, april 2014," in *Proceedings of the 2nd International Conference on Learning Representations, ICLR 2014*, Banff, Canada, January, 2014.

[128] I. Sachdeva, S. Ramesh, U. Chadha, H. Punugoti, and S. K. Selvaraj, "Computational AI models in VAT photo-polymerization: a review, current trends, open issues, and future opportunities," *Neural Computing and Applications*, vol. 34, no. 20, pp. 17207–17229, 2022.

[129] A. Bhat, R. S. Elsen, D. Abishai et al., "Prediction and experimental verification of distortion due to residual stresses in a Ti-6Al-4V control arm plate," *Advances in Materials Science and Engineering*, vol. 2022, Article ID 5211623, 11 pages, 2022.